Arctic Atmospheric Rivers:
Linking Atmospheric Synoptic Transport, Cloud Phase, Surface Energy Fluxes and Sea-Ice Growth

Ola Persson

Cooperative Institute for the Research in the Environmental Sciences, University of Colorado, Boulder, Colorado, USA; NOAA/ESRL/PSD, Boulder, Colorado, USA

2233 UTC Sep 23 (YD266)
Winds: 12.2 m/s, 208°

Contributions from: M. D. Shupe, D. Perovich, and A. Solomon

1) Link Arctic ARs to mid-latitude ones – extension of mid-latitude ARs through Arctic gateways
2) Characteristics comparison: moisture content/transport
3) Impact comparison: surface precipitation, radiation, SEB, ice growth
4) Detailed examples – SHEBA midwinter; SHEBA spring; ACSE summer

Moisture Transport by Atmospheric Rivers (Zhu and Newell 1998)

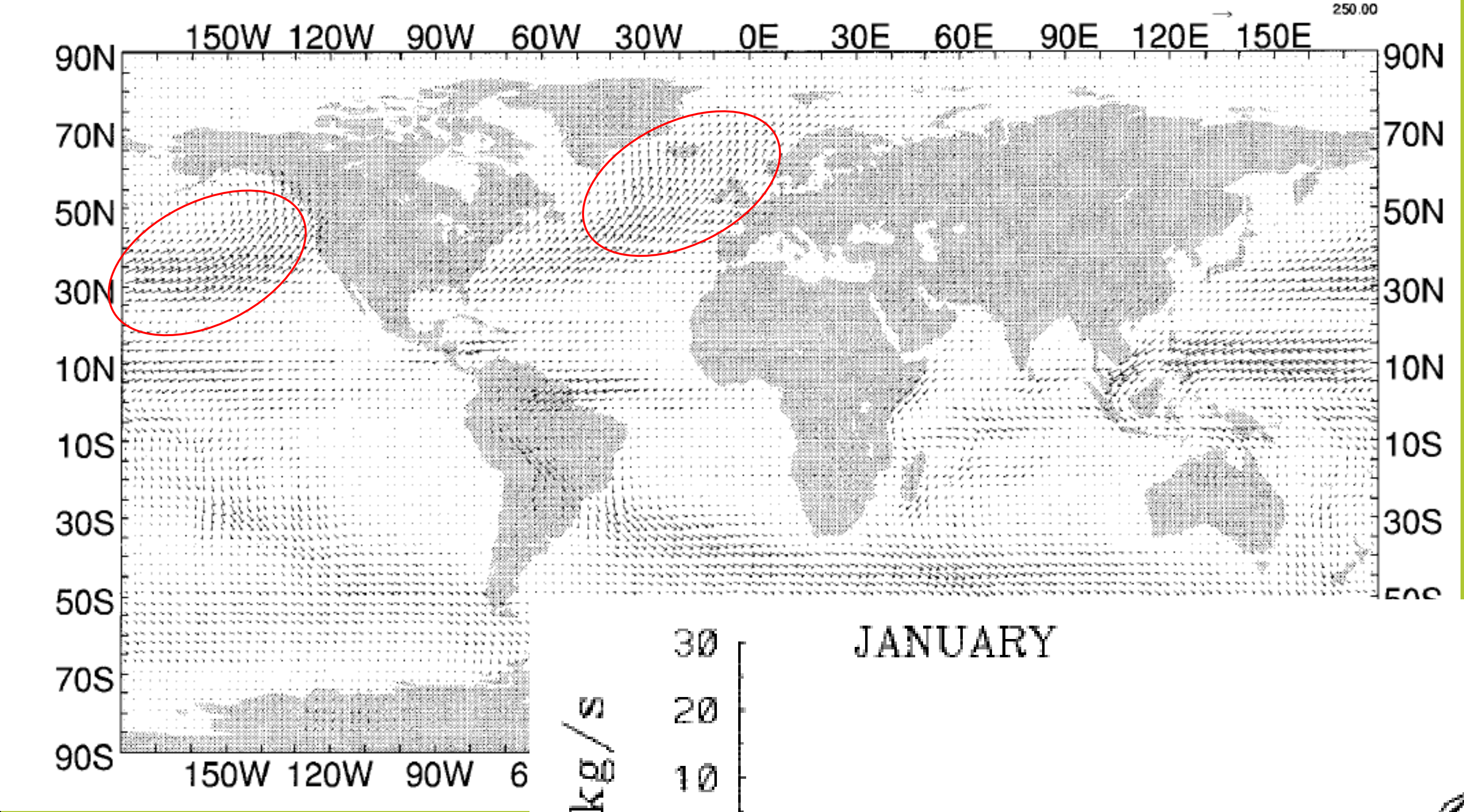

River fluxes (kg m^{-1} s^{-1}) for January 1992, 1995, and 1996. Sample vector magnitude illustrated in upper-right corner.

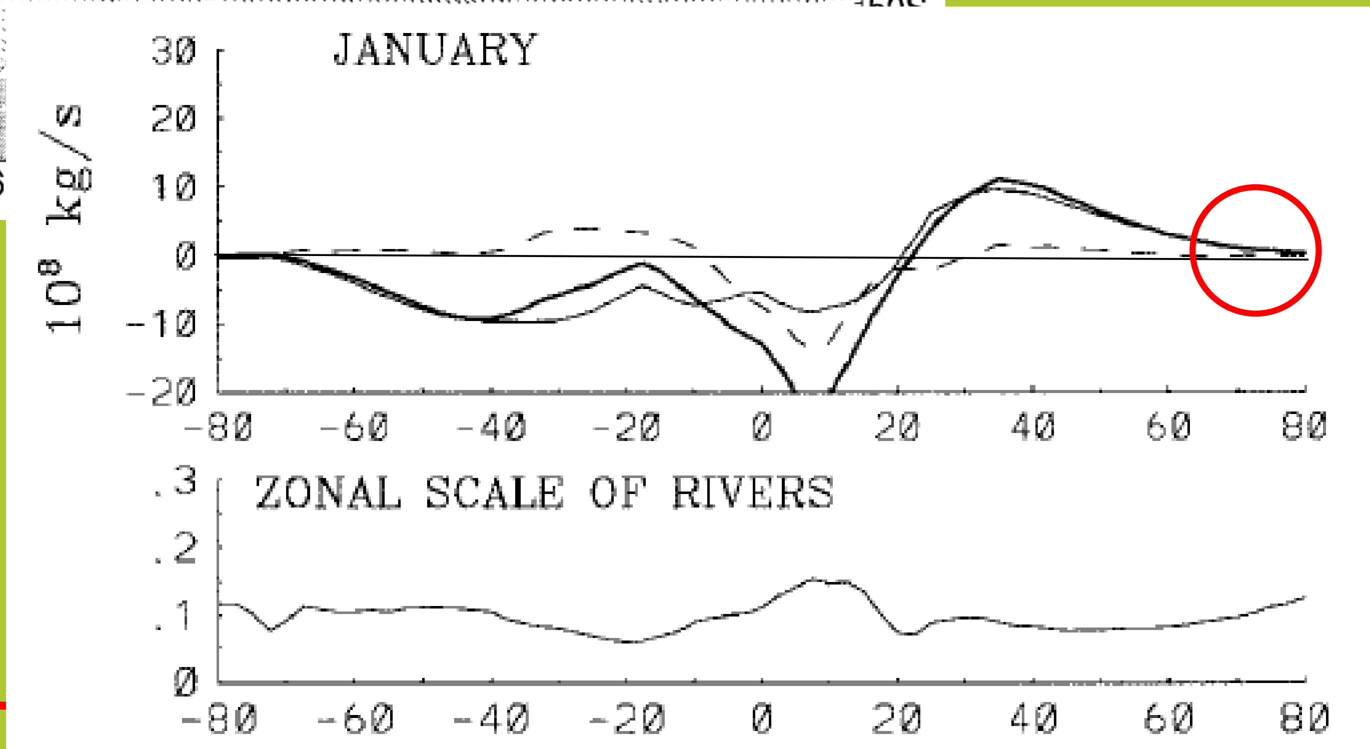

Northward moisture flux by rivers, broad fluxes, and their totals. Rivers, thin solid line; broad fluxes, dashed line; and total flux, thick solid line. Units are 10^8 kg s^{-1}. (Top panel) January 1992, 1995, and 1996; (second panel) zonal scale of rivers for January 1992, 1995, and 1996; (Zhu and Newell,1998).

The Arctic

Typical Temperature Profiles Over Arctic Sea Ice (Persson and Vihma 2016)

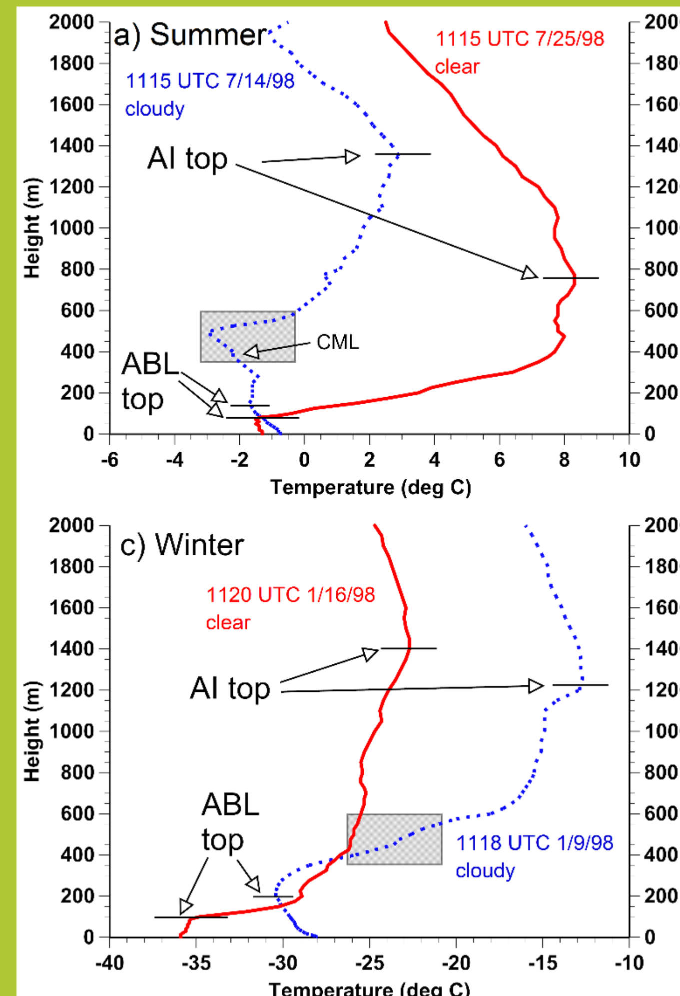

SLP Associated with Moisture Pathways into the Arctic (Woods et al 2013; ERA-I)

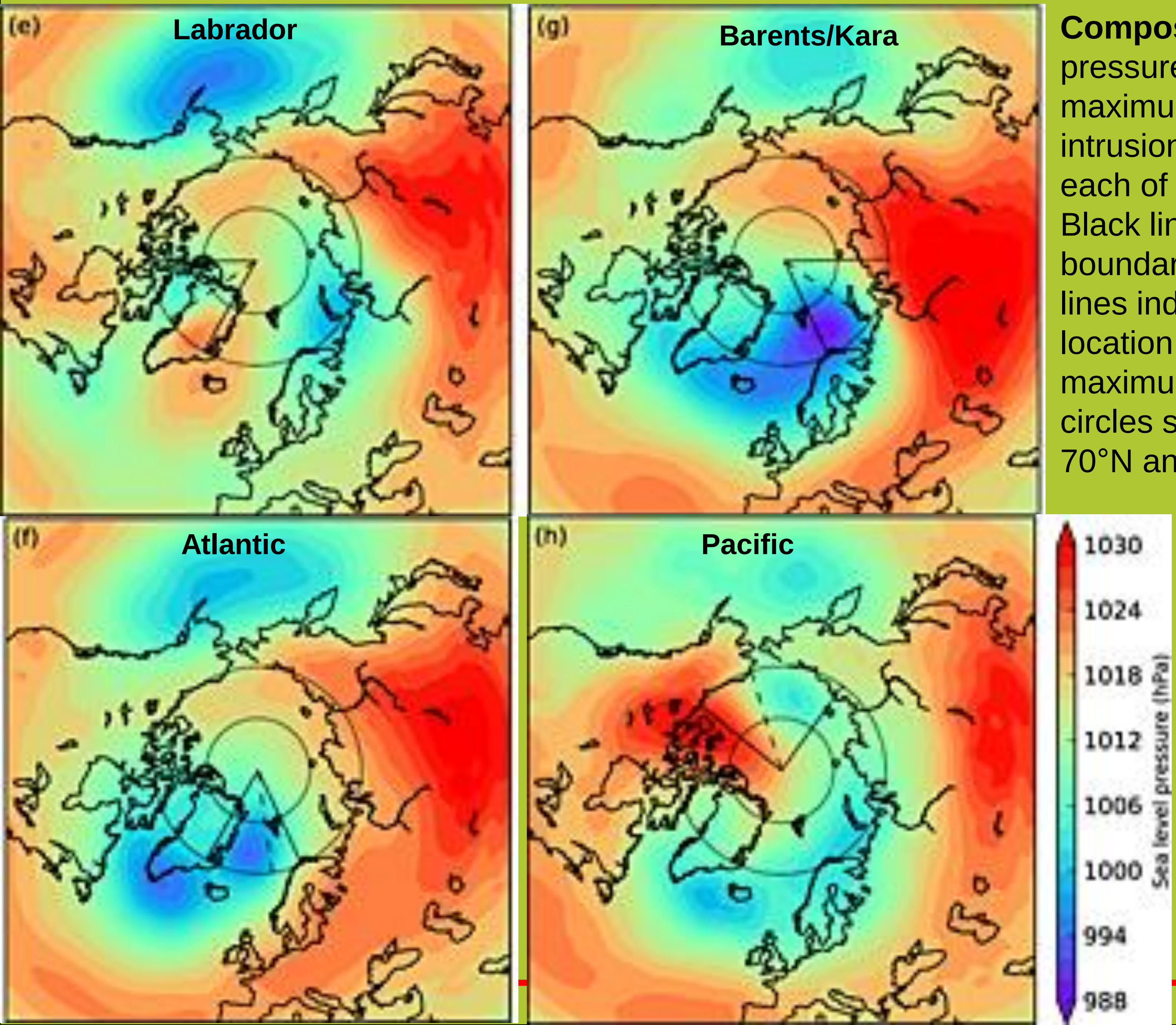

Composites of sea level pressure at the time of maximum intensity for intrusions occurring within each of the four sectors. Black lines show the sector boundaries. Dashed black lines indicate the median location of the intrusions at maximum intensity. Dotted circles show latitude lines at 70°N and 80°N.

Moisture Pathways into the Arctic

Woods et al 2013; GRL; ERA-I

(a) Zonal cross section along 70°N showing the **climatological poleward moisture flux** during winter from 1990 to 2010.

(b) **Proportion of total poleward moisture transport across 70°N** from 1990 to 2010 contributed by vertically integrated moisture fluxes in 75 Tg d^{-1} deg^{-1} by 5° longitude bins. Dashed and solid black lines mark the 50th and 90th percentile values of vertically integrated poleward fluxes, respectively. Solid red line indicates the threshold value of flux used to detect intrusions in the algorithm.

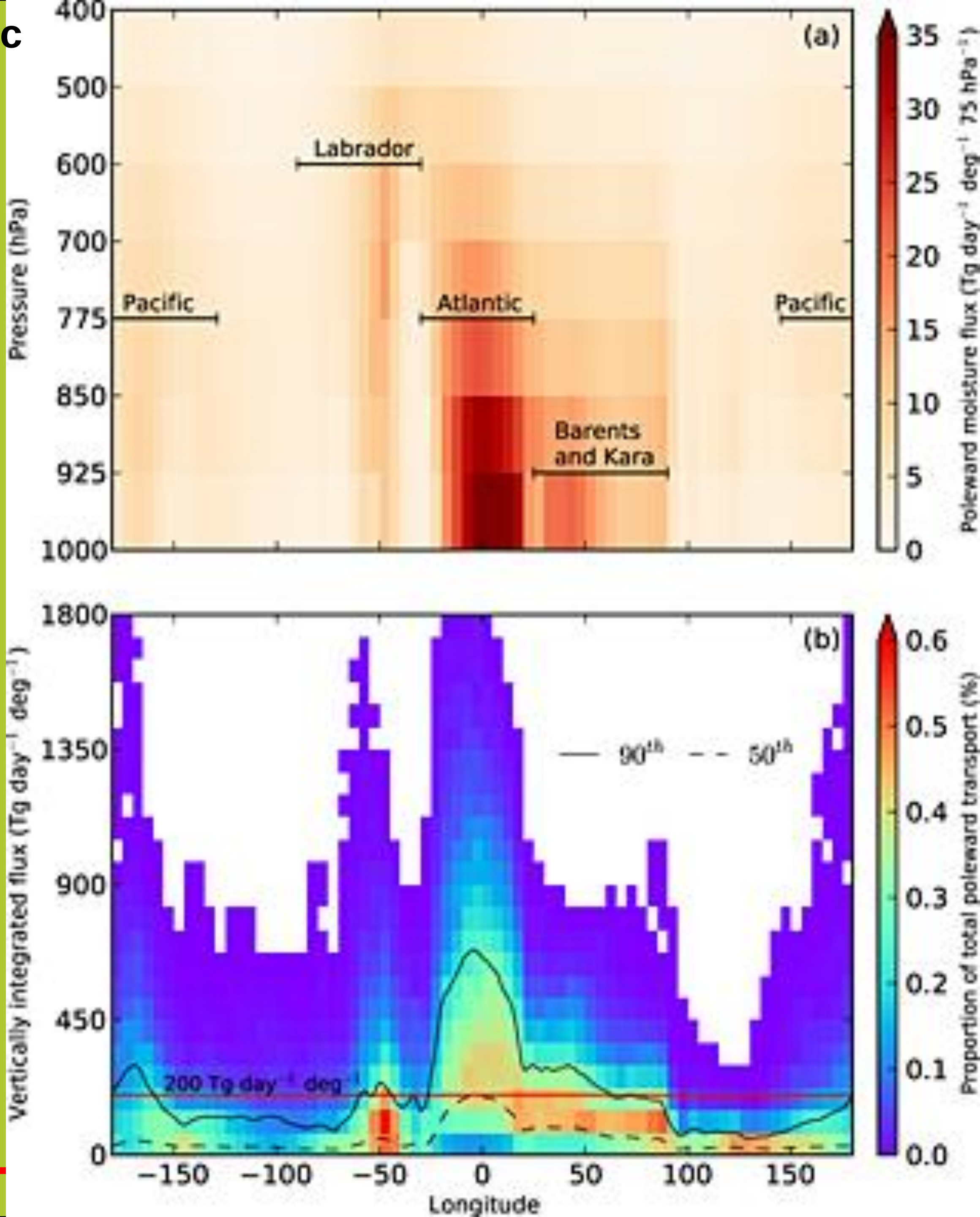

Moisture Intrusion Example – Atlantic Sector

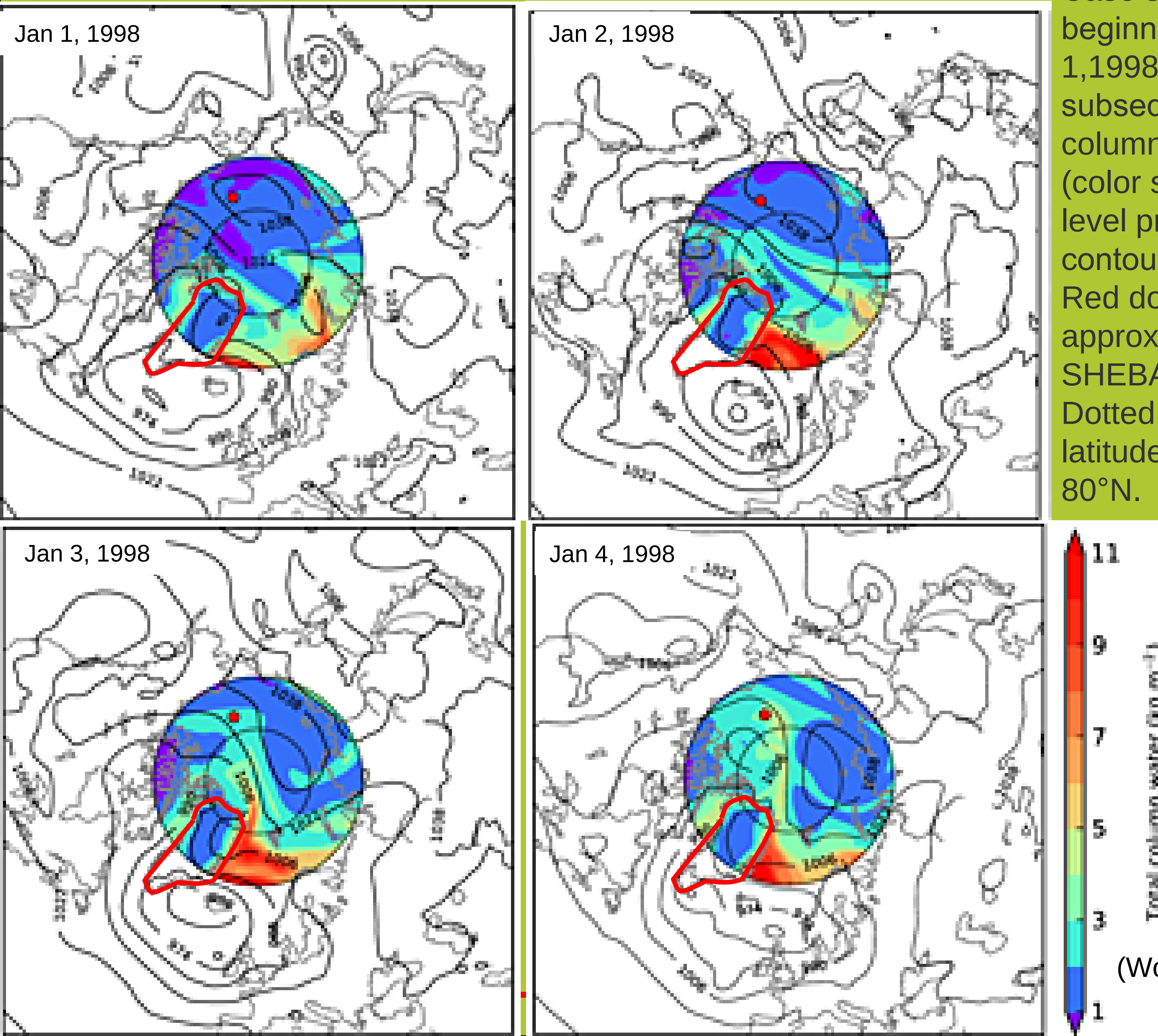

Case study of an intrusion beginning at 00 UTC Jan 1,1998 and followed for subsequent 3 days. Total column water over ocean (color shading) and sea level pressure (black contours every 16 hPa). Red dot denotes approximate location of SHEBA at this time. Dotted circles show latitude lines at 70°N and 80°N.

(Woods et al 2013; GRL)

ERA-40: Water Vapor Mixing Ratio, winds at 1500 m; Jan 2 - 5, 1998

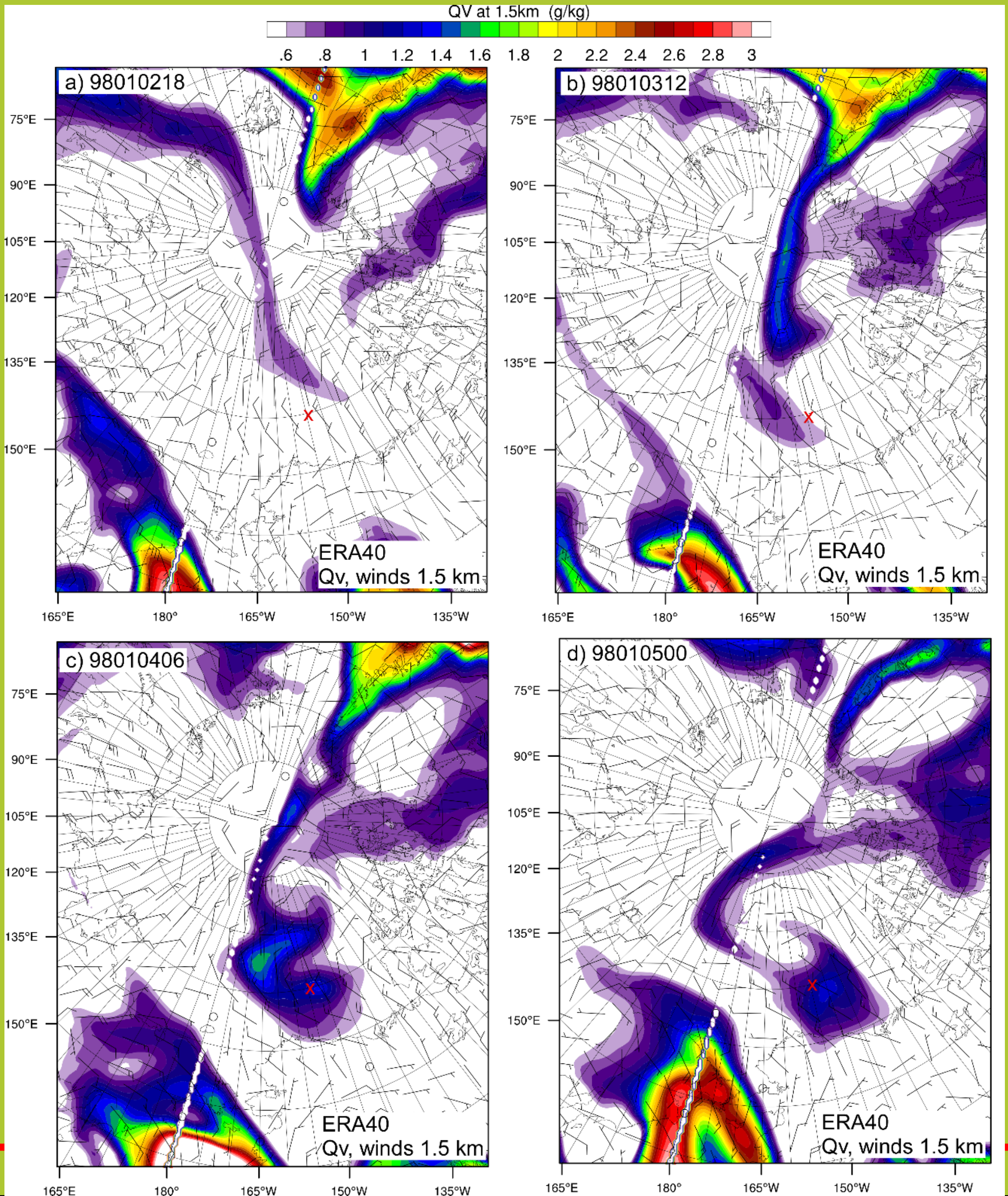

(Persson et al 2016)

Moisture Intrusion from Atlantic Gateway

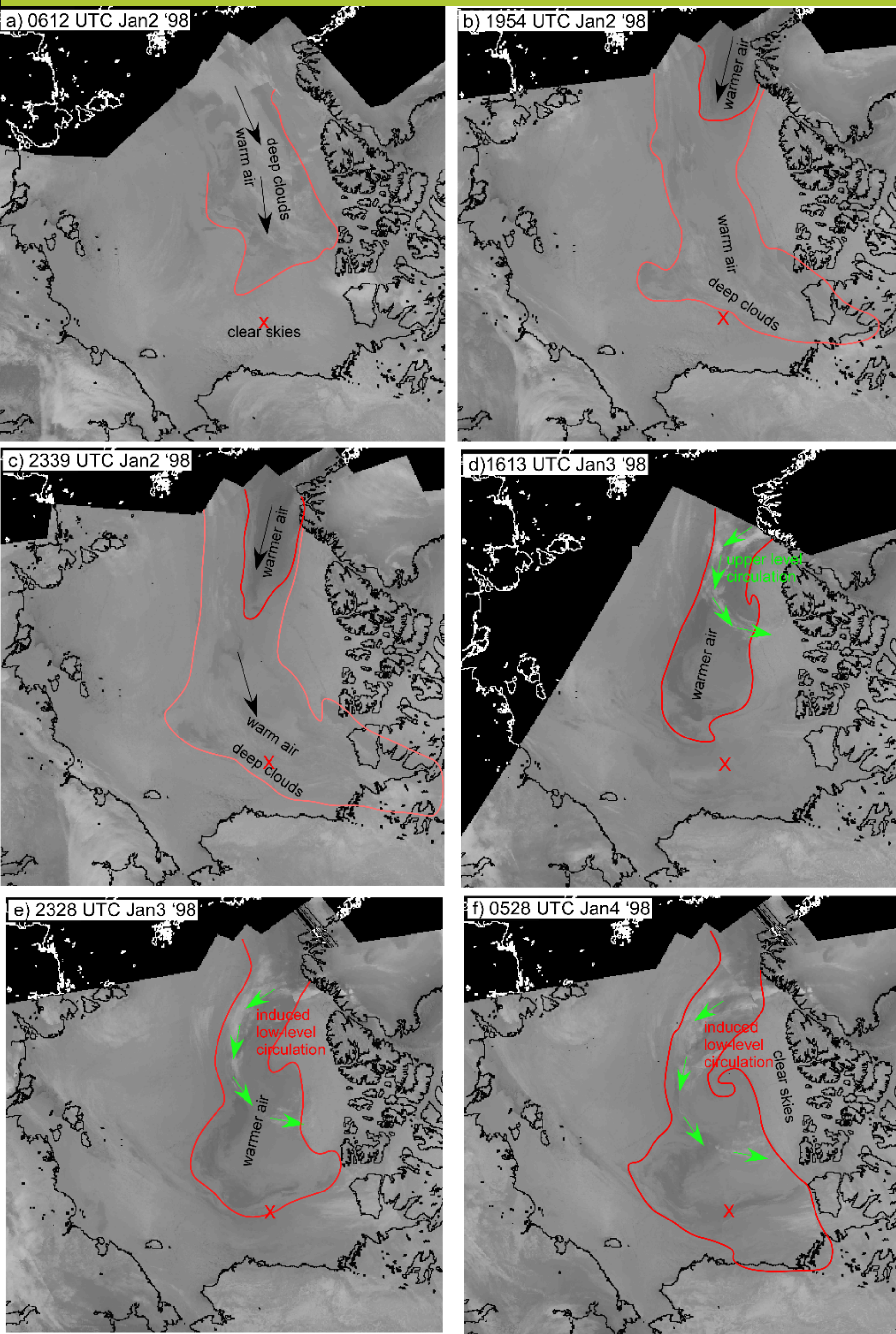

Moisture Intrusion from Pacific Gateway

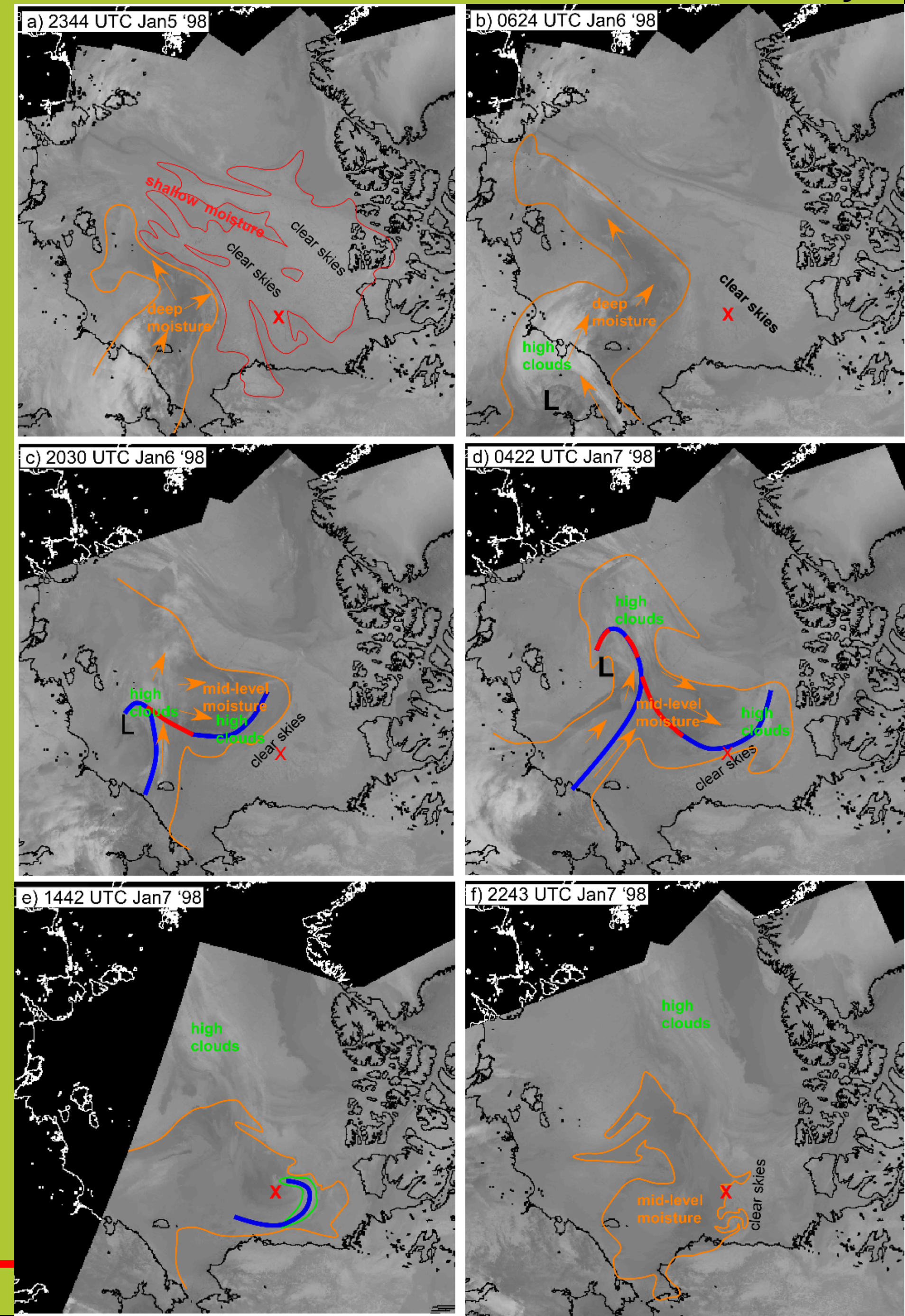

Moisture Intrusions Reaching SHEBA Observation Site

- early Jan 1998
- suite of in-situ and remote sensors, including 2-4X daily rawinsondes

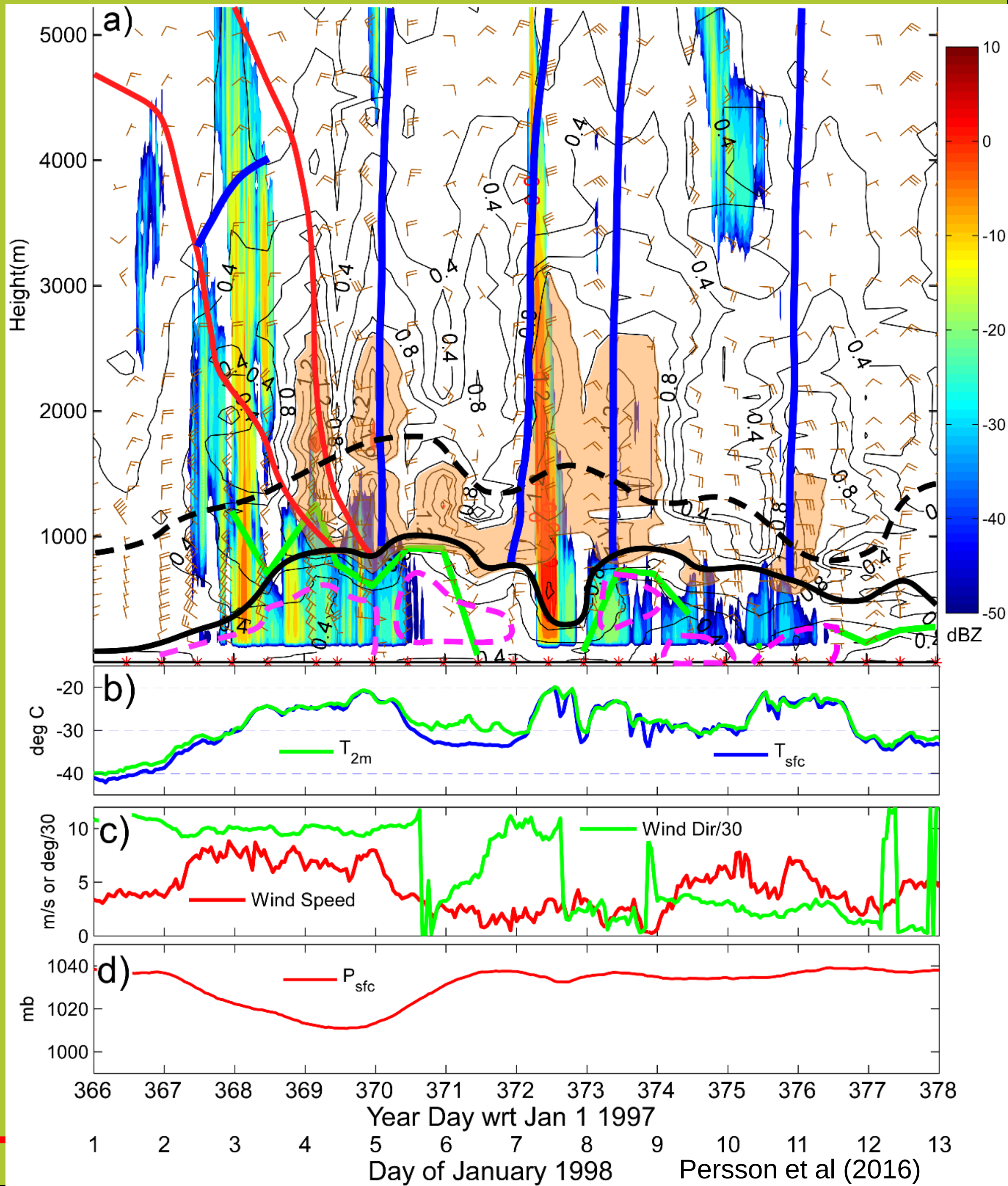

1) Long-distance free tropospheric (above AI) advection of heat and moisture

2) Associated clouds (esp. with liquid) have strong impact on LW_d, F_{net}, and T_s

3) Thermal structure in snow and ice respond strongly to synoptic/mesoscale atmospheric events and presence of liquid water in clouds

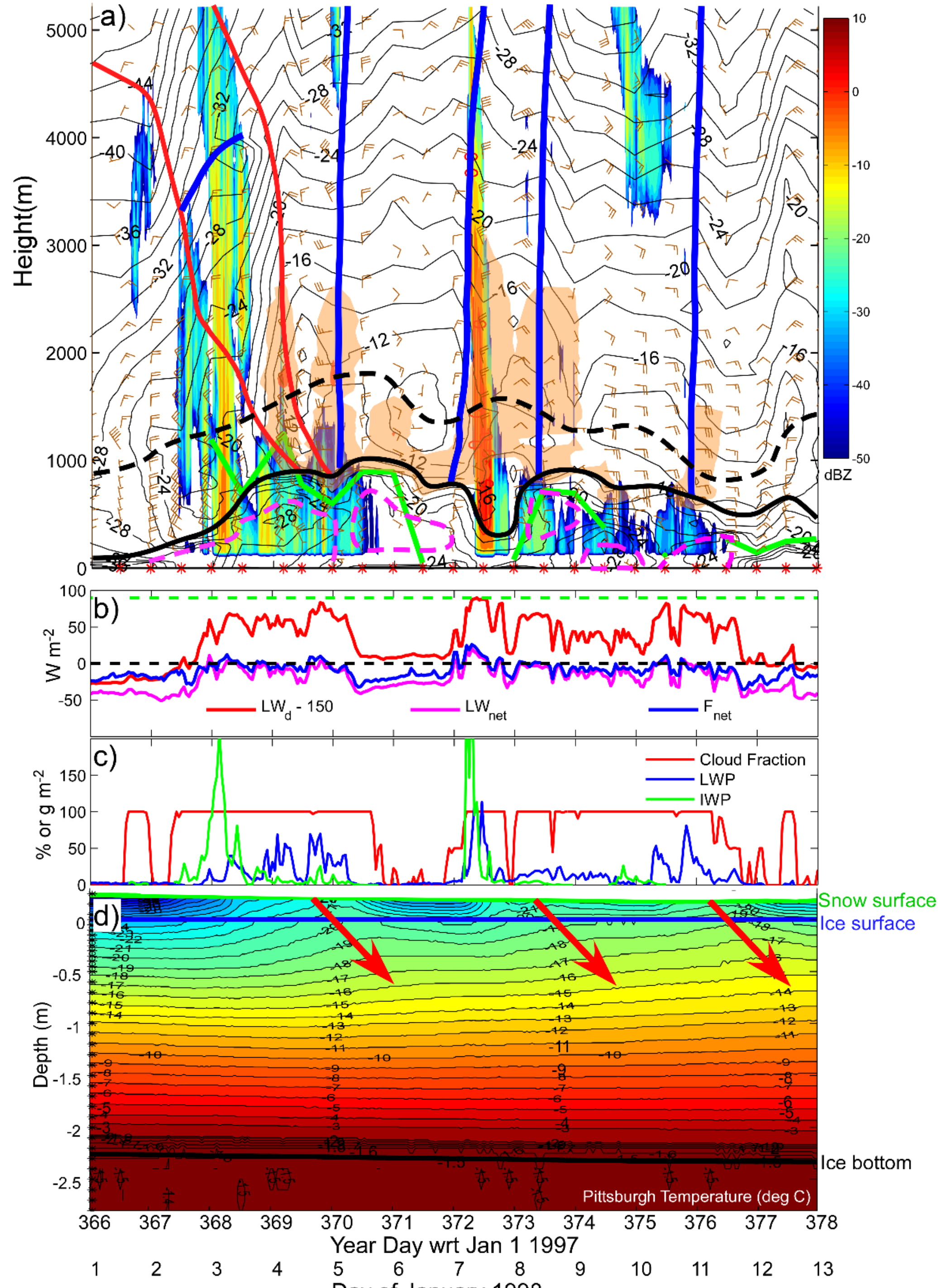

Observed Responses to Radiation Changes over Arctic Sea Ice

SHEBA Polar Night (Nov. 7, 1997 – Feb. 2, 1998; No solar radiation)
Beaufort Sea – Multi-year Arctic sea ice

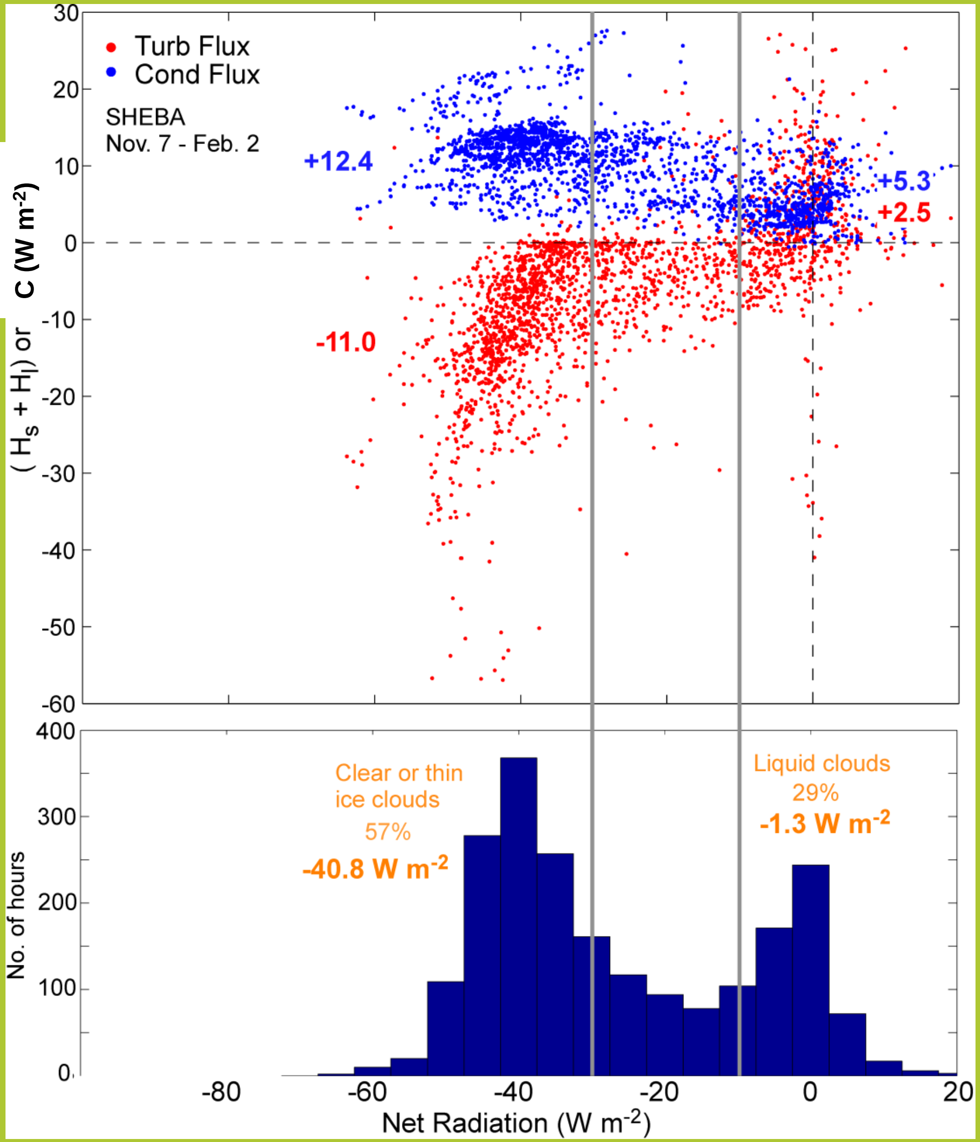

Observations clearly show clouds and CLW also impact $H_s + H_l$ and F_0

Process Relationships:

$F_{net} \approx LW_{net} - (H_s + H_l) + C;$

$\mathbf{H_s + H_l}$ **vs** $\mathbf{LW_{net}}$**,** $\mathbf{C}$ **vs** $\mathbf{LW_{net}}$

Clear skies
- surface warmed by both H_s+H_l and C
- F_{net} ~ -17.5 W m^{-2}

Sea-Ice Heat Conduction – SHEBA Observations (Nov 16, 1997 - Feb 28, 1998; Persson et al 2016)

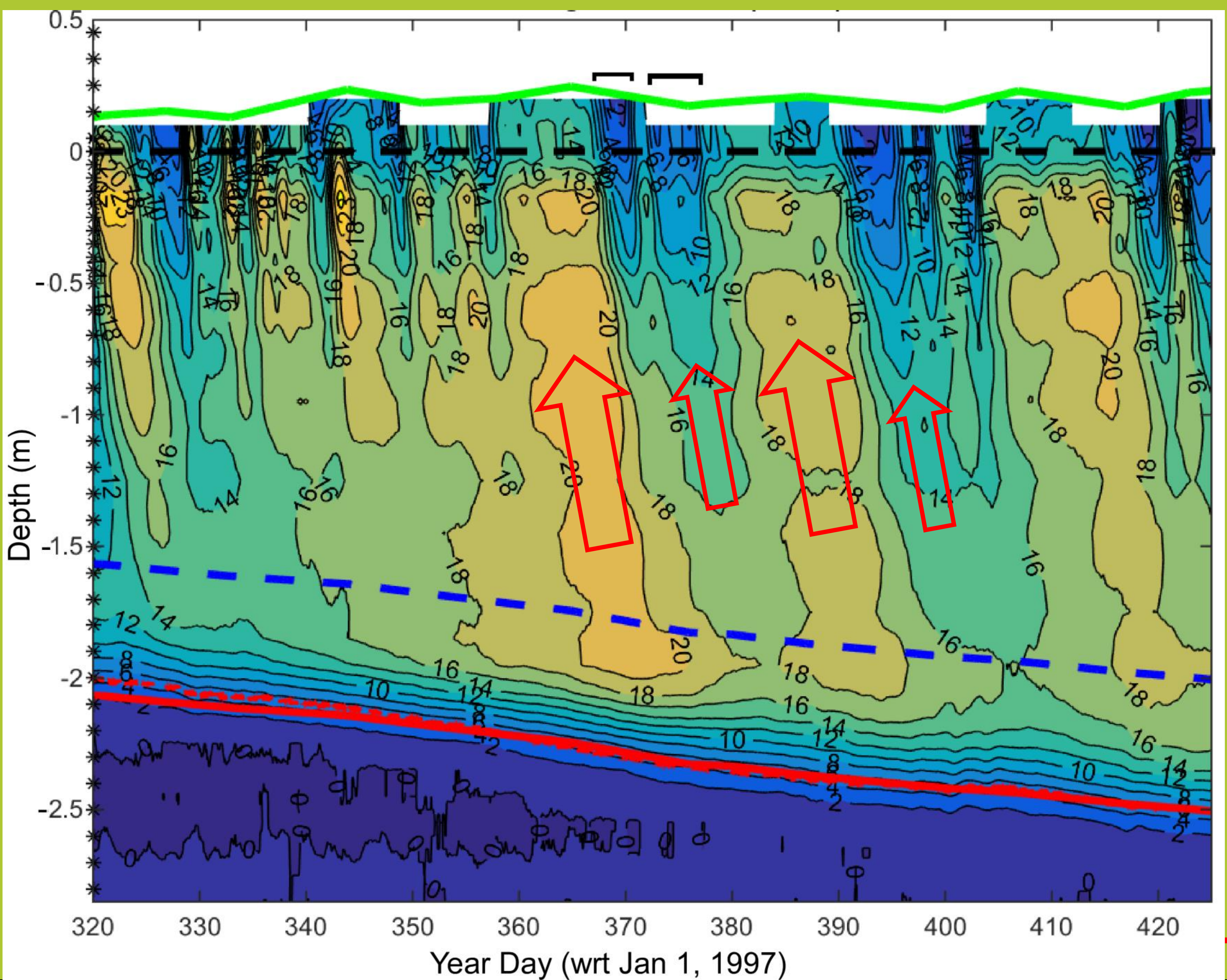

How Arctic Moisture Intrusions Impact Sea Ice Growth

(Persson et al 2016)

Cloud liquid water path

Surface net energy flux

Snow surface conductive energy flux

In-ice conductive energy flux

Ice growth rates – flux estimates

Ice growth rates – observed

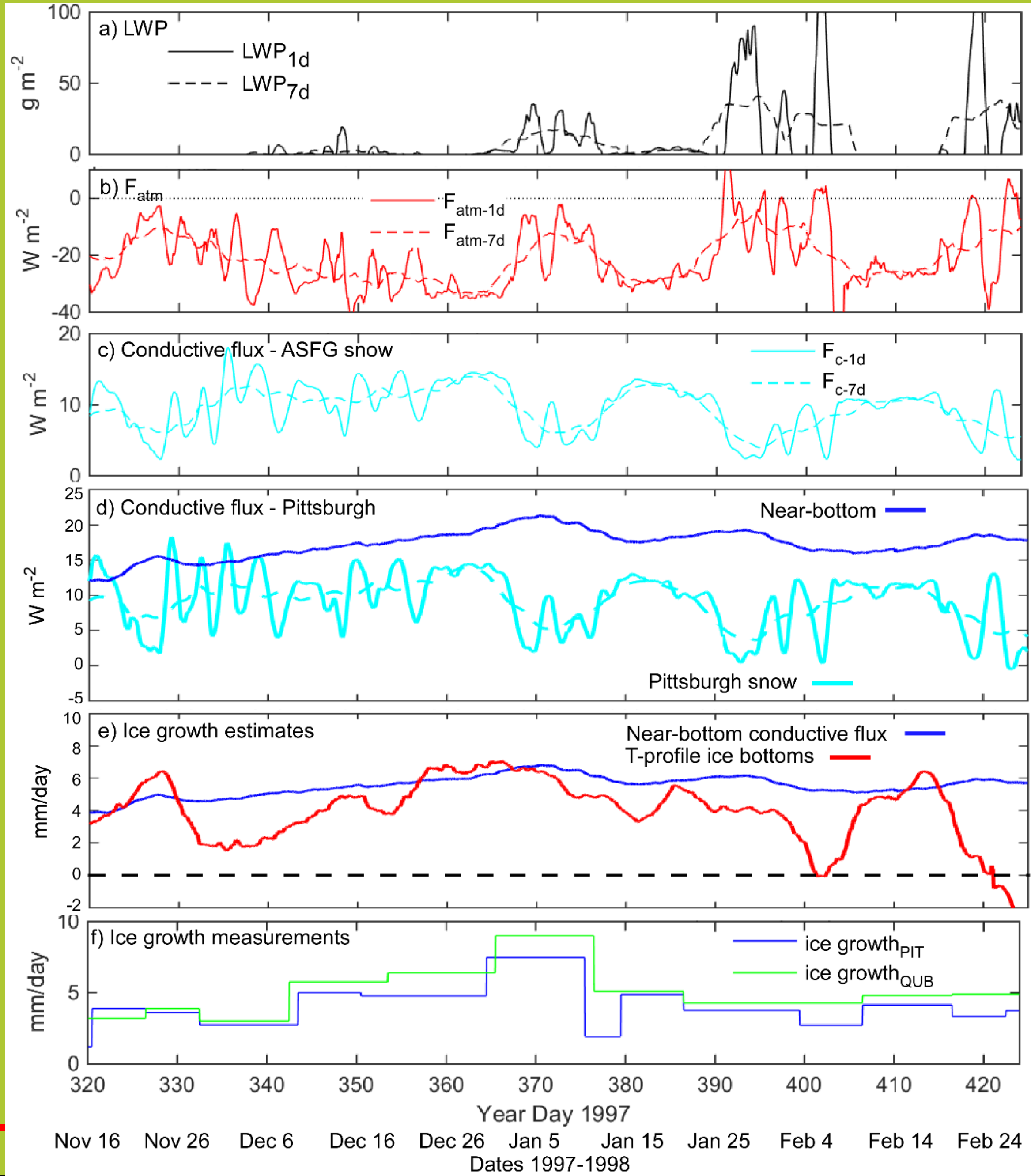

Impacts of Moisture/Heat Intrusions over Sea Ice

Snow cover,
ice temperatures (color),
ice outlines
Perovich et al (2003)

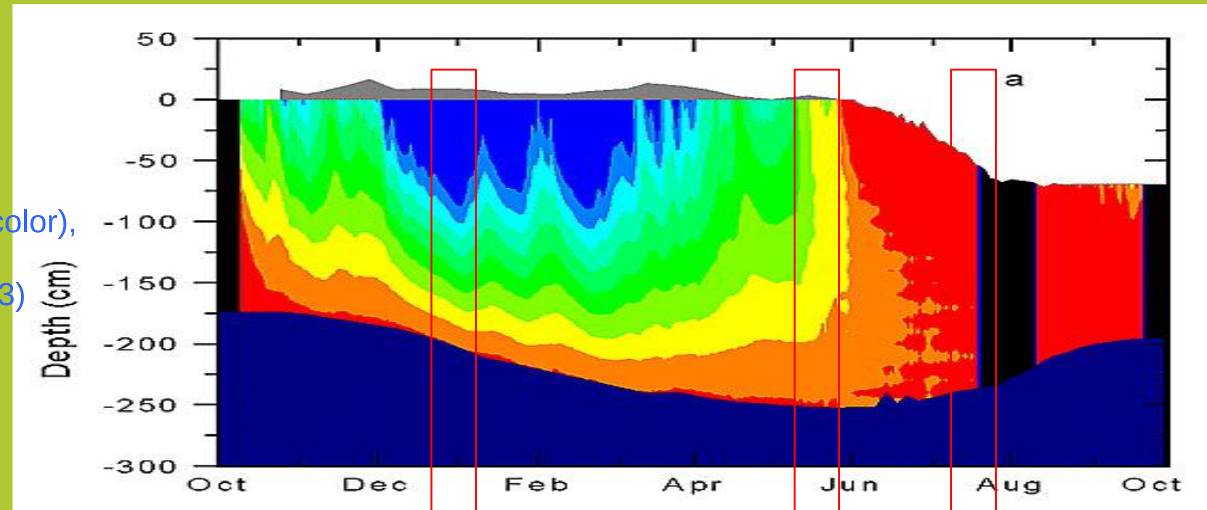

Impact on all SEB terms, but particularly LW_d

3-day running means of SEB terms, ice-surface melt, albedo, sfc T
Persson (2012)

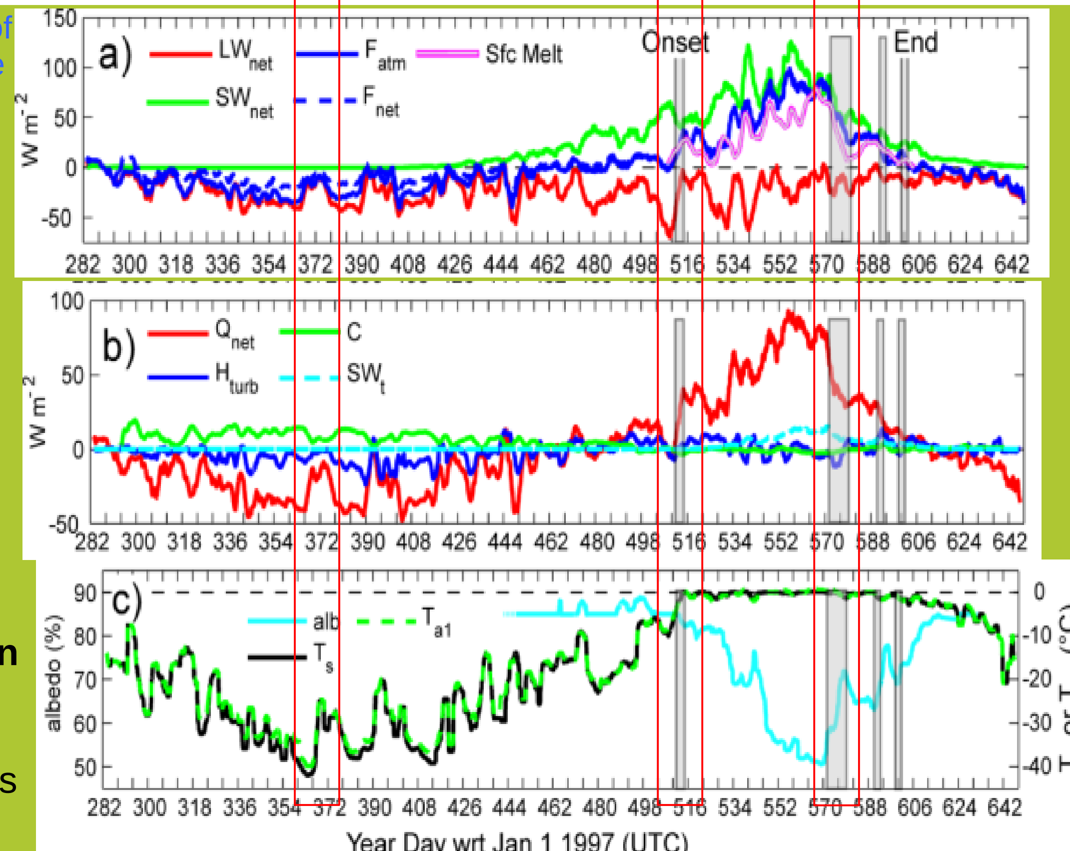

Non-Summer Seasons (T_s can vary)
- Large near-surface T_a increases
- Can trigger onset of summer melt

Summer Season (T_s fixed at melting point)
- Can enhance surface melt

Intrusions have potential significant impact on annual F_{tot}:
a) Increasing/decreasing number of events
b) Increasing/decreasing F_{tot} amplitudes of events

CONCLUDING REMARKS

Mid-latitude Atmospheric Rivers continue as moisture intrusions into the Arctic

- several gateways, but esp. Atlantic (Svalbard area)
- moisture content less (often significantly) (1-11 g/kg; < 3 cm IWV)
- airflow weaker
- hence moisture transport significantly weaker ⇨ "Atmospheric Creeks"?

Arctic ACs have major impacts on sea-ice surface, primarily through LW_d

- large near-surface temperature increases (non-summer seasons)
- trigger melt-season onset; enhance melt during melt-season
- near-surface meteorology (e.g., fog, precipitation)

Changes in frequency/strength of Arctic moisture intrusions potential major impact on near-surface climatology and sea-ice evolution

Atmospheric river system flows <u>opposite</u> to the analogous terrestrial river system

- terrestrial system has many small creeks feeding rivers, which eventual feed the large global water reservoir (oceans)
- atmospheric system has moisture flow from the large global reservoir (tropical troposphere) into large "atmospheric rivers", which are then depleted and eventually form a similar number of Arctic "atmospheric creeks"
- terrestrial system primarily driven by gravity and earth's topography; atmospheric system driven by global general circulation and Clausius-Clapyron equation

Melt Onset Triggered by Heat/Moisture Intrusion

May 26-30, 1998; Persson (2012)

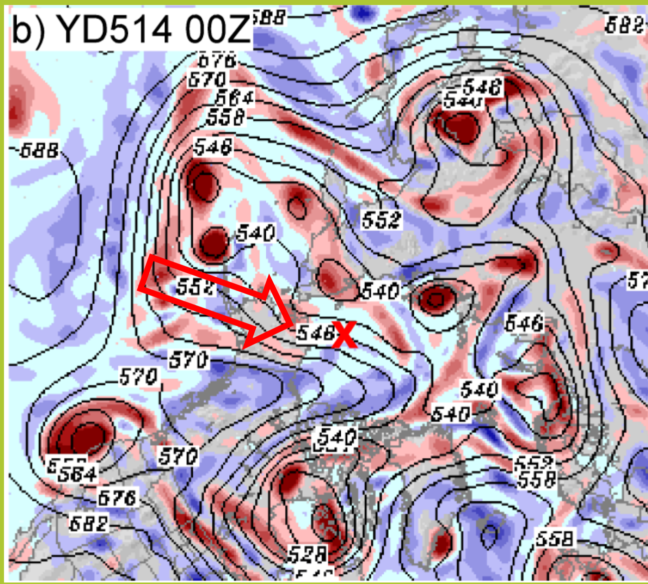

Eddy on 500 mb circumpolar flow provides intrusion meridional flow

Radar reflectivity, θ_e, T, q_v, and frontal analysis

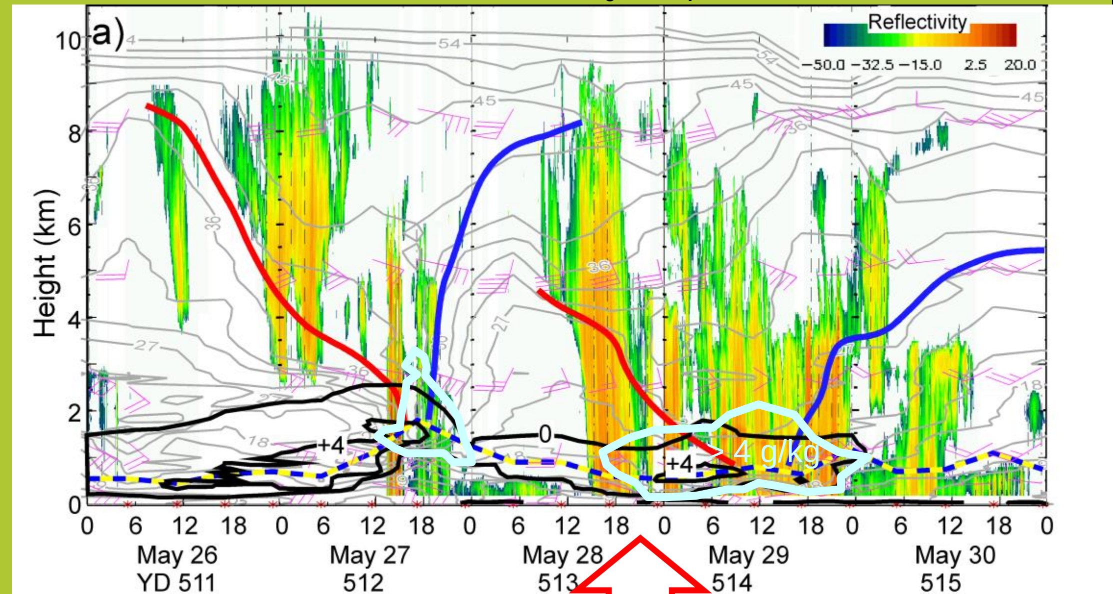

Surface met and SEB evolution

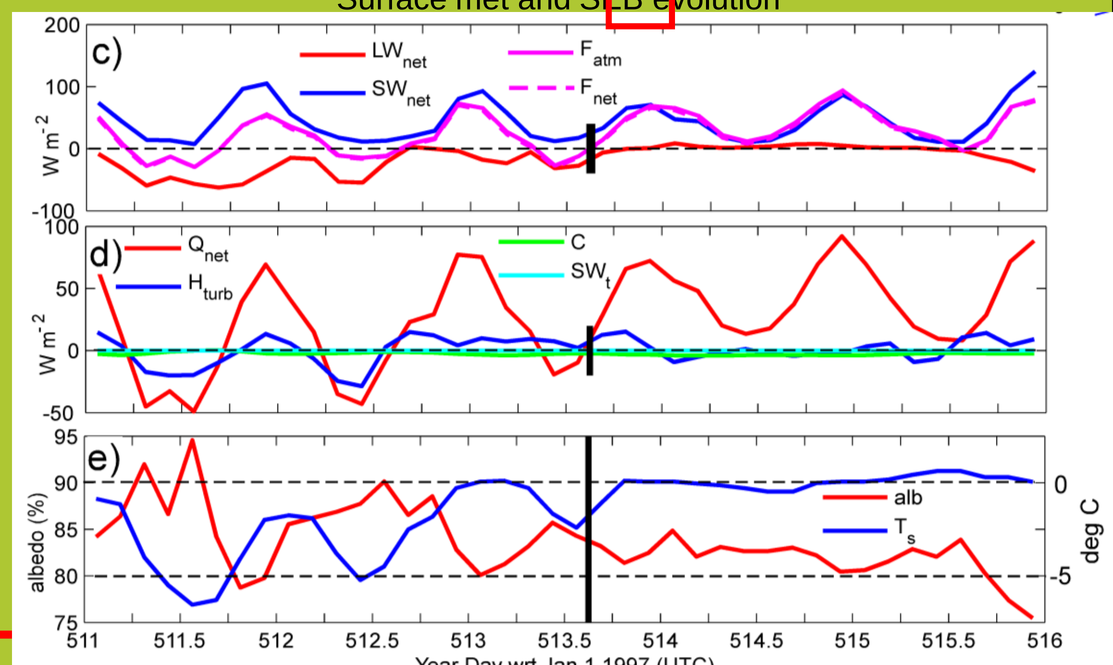

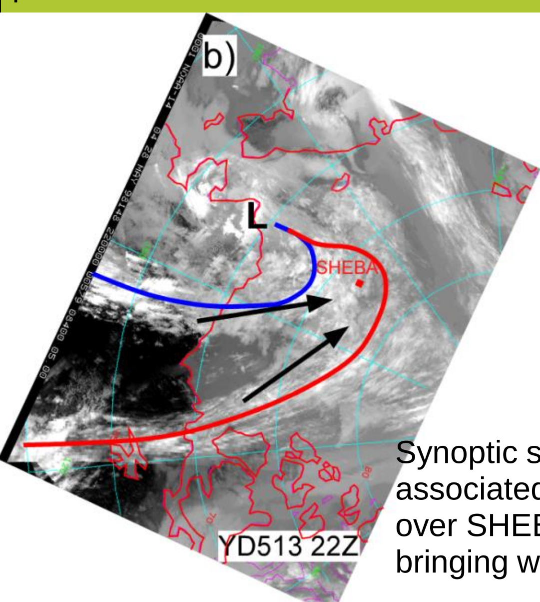

Synoptic storm & associated fronts pass over SHEBA site, bringing warm, moist air

Very Strong Arctic Moisture and Heat Intrusion

E. Siberian Sea; 1-7 Aug, 2014 (Tjernström et al 2015)

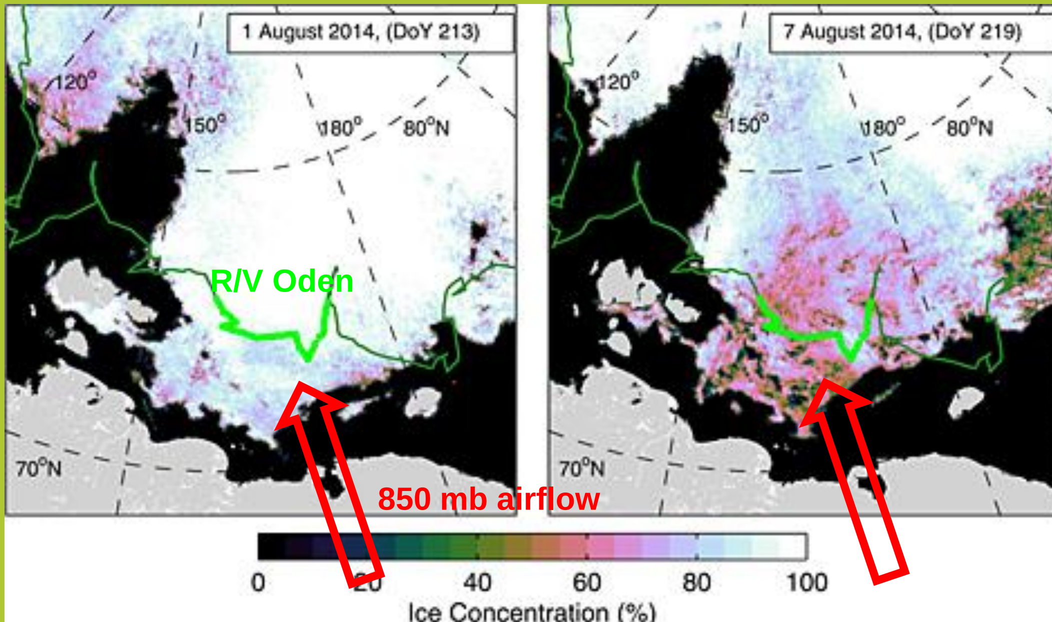

Select R/V Oden Observations

Variables related to clouds and daily averaged surface energy fluxes. Top: PWV (cm); Middle: horizontal visibility (km); Bottom: net longwave (red) and solar (blue) radiation, and sum of turbulent sensible and latent heat fluxes (green), and total energy flux (black); Positive energy fluxes are downward. Upwelling and net solar radiation and total energy flux assume an albedo of 60%; dotted lines indicate ±10% about this. Shaded region indicates period with positive surface net longwave radiation.

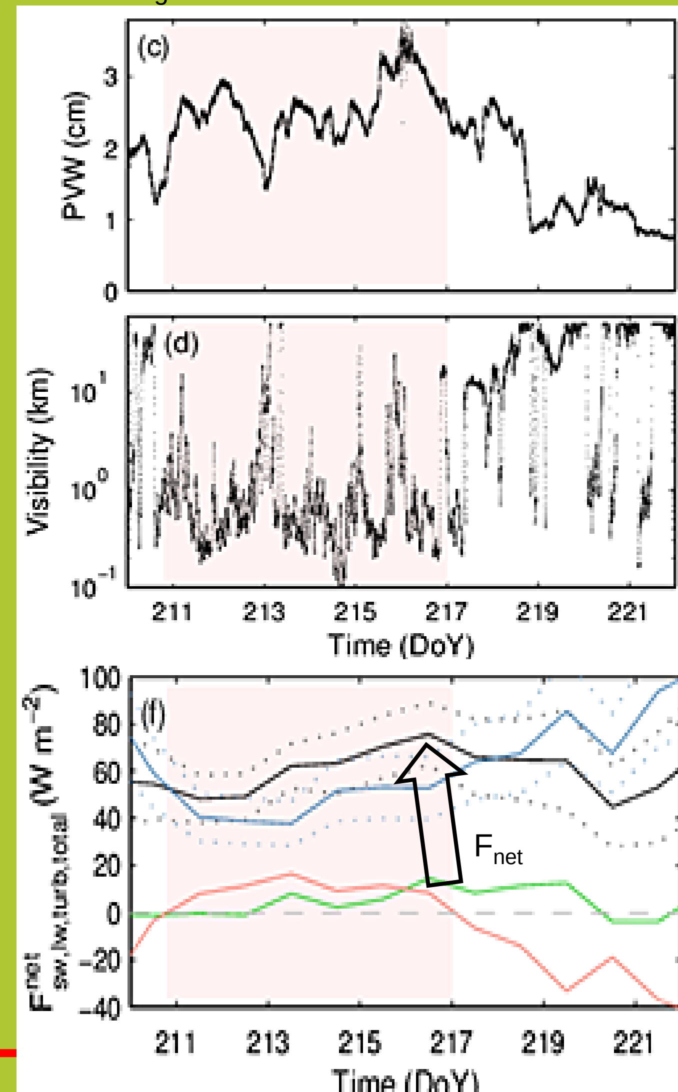

R/V Oden Serial 6-h Rawinsondes

Temperature (deg C) Absolute Humidity (g/kg)

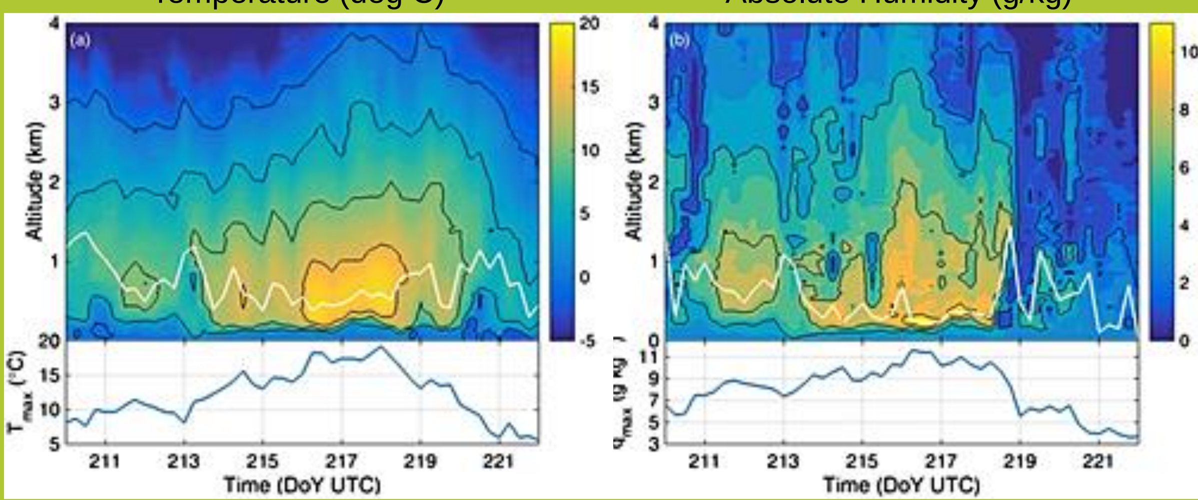

Moisture Intrusion with Storm/Precipitation

Near North Pole, ASCOS, Aug 12-13, 2008; Persson (2010)

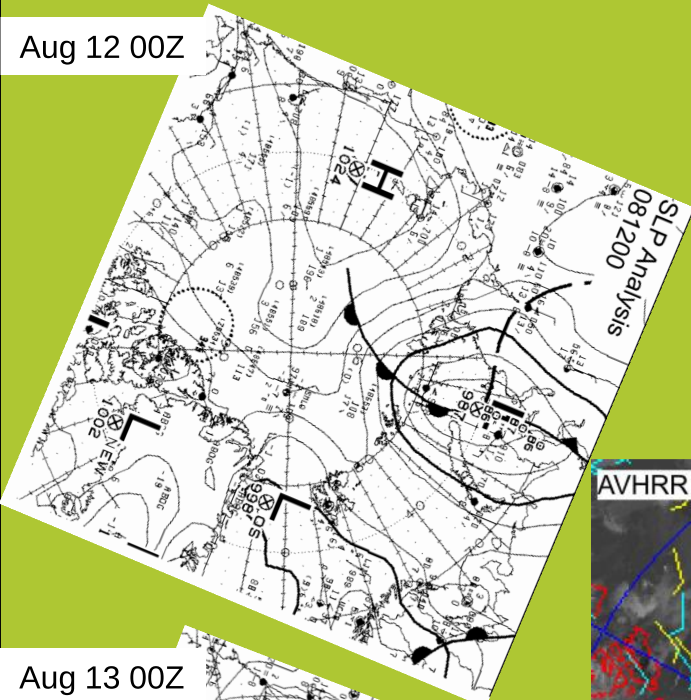

Aug 12 00Z

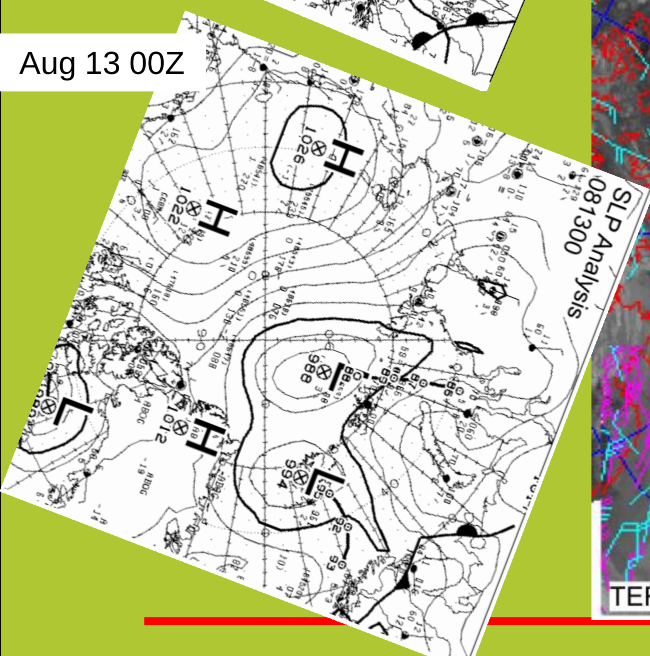

Aug 13 00Z

Canadian Weather Service sea-level pressure analyses at a) 00 UTC Aug. 12, b) 12 UTC Aug. 12, c) 00 UTC Aug. 13, and d) 12 UTC Aug. 13. The Oden is the reporting station at 87.5° N, 2° W.

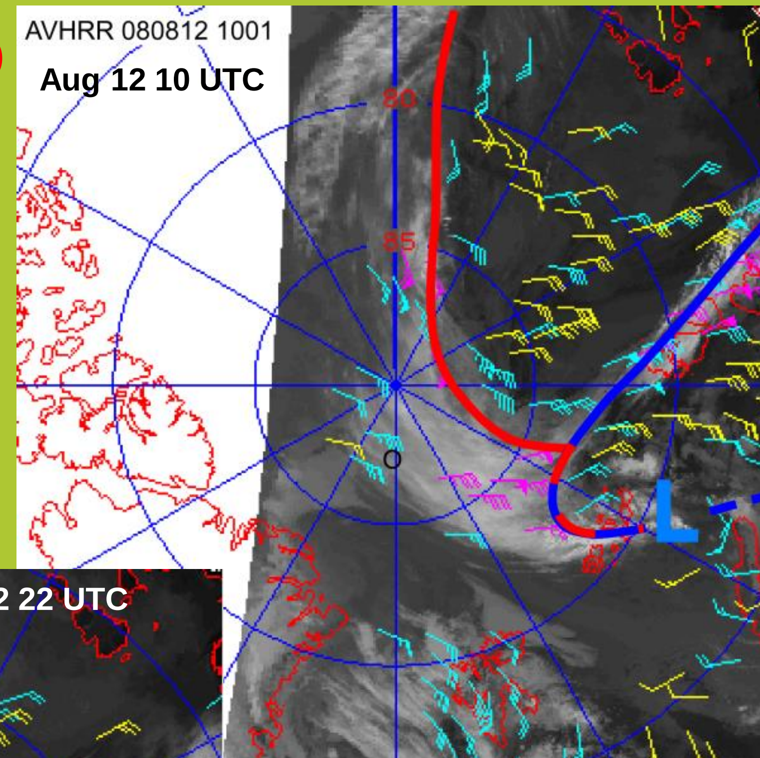

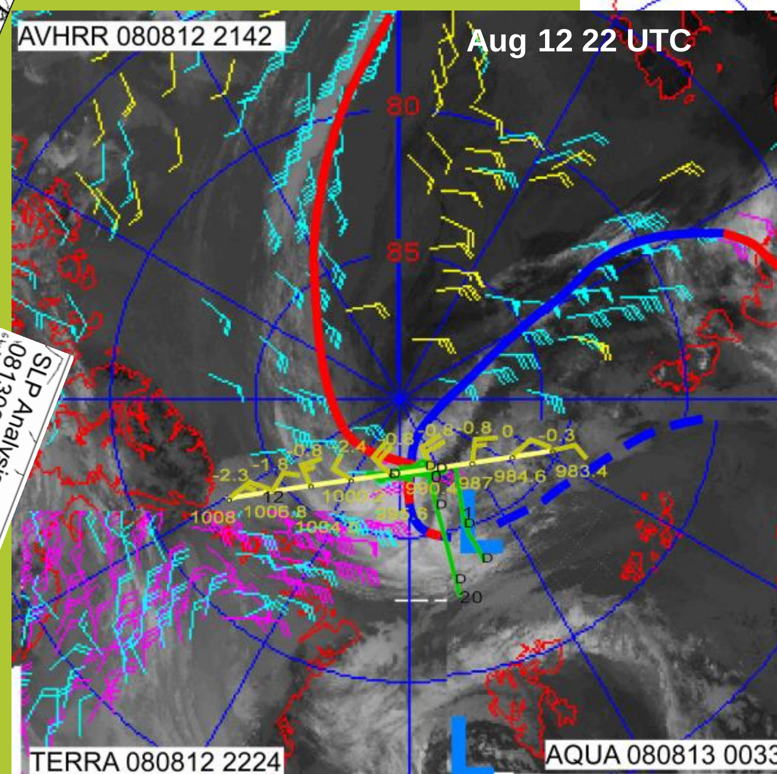

Sequence of AVHRR satellite images showing the synoptic evolution. The satellite-derived winds and the surface frontal features are shown in each image. The tracks of the DC-8 (green) and Oden (yellow) are shown in b) using a system phase velocity of 14.5 m s^{-1} from 81°.

Moisture Intrusion with Storm/Precipitation: Thermodynamic/Kinematic Structure

Near North Pole, ASCOS, Aug 12-13, 2008; Persson (2010)

Time-height cross section of a) θ_e (deg C), wind barbs, and S-band SNR; b) temperature (deg C) and S-band vertical velocity; and c) mixing ratio (g kg^{-1}) and S-band spectral width.

Each panel is overlaid with a frontal analysis based primarily on θ_e (heavy red, blue, and purple lines), theDC-8 flight track data (heavy black line), radiosondes (red stars on abscissa & vertical dashed lines), and dropsondes (vertical dashed blue lines). The heavy red isopleth in b) is the 0° C isotherm, and the heavy magenta line shows the location of a strong inversion.

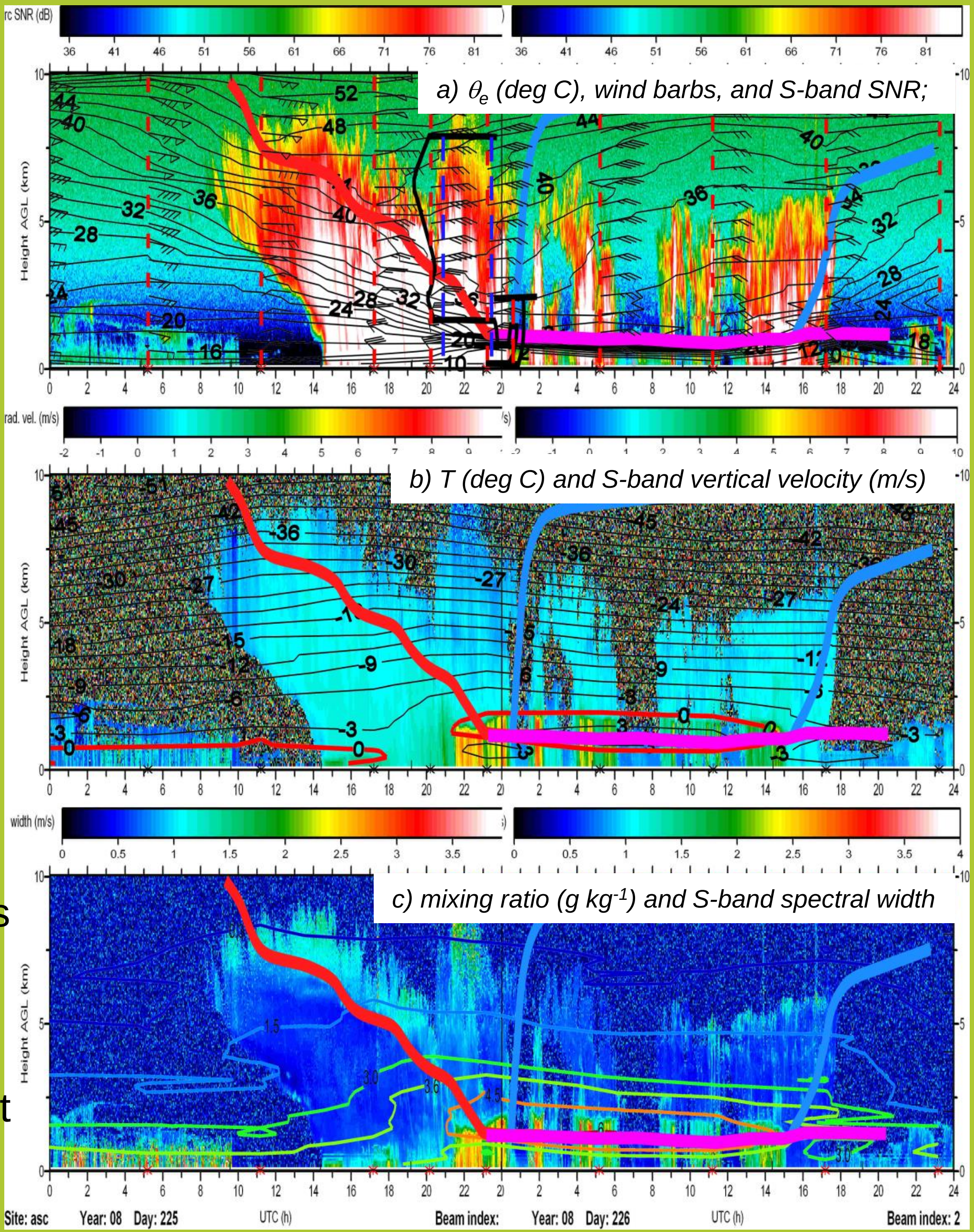

Main Points

1) Classical occluded frontal system, with warm/moist advection in narrow warm sector above surface inversion
2) Post-frontal warm air separated from surface by inversion
3) Deep clouds and precipitation primarily associated with warm-front
4) Elevated warm-air advection producing period of surface freezing rain and sleet
5) Turbulence near top of warm-frontal clouds likely producing convective generating cells for warm-frontal precipitation and possibly supercooled liquid water
6) Classical occluded frontal structure (except low-level inversion); clouds dynamically forced

Clouds Triggering Melt

Observed and simulated temporal evolution of the July 2012 surface melting event at Summit.

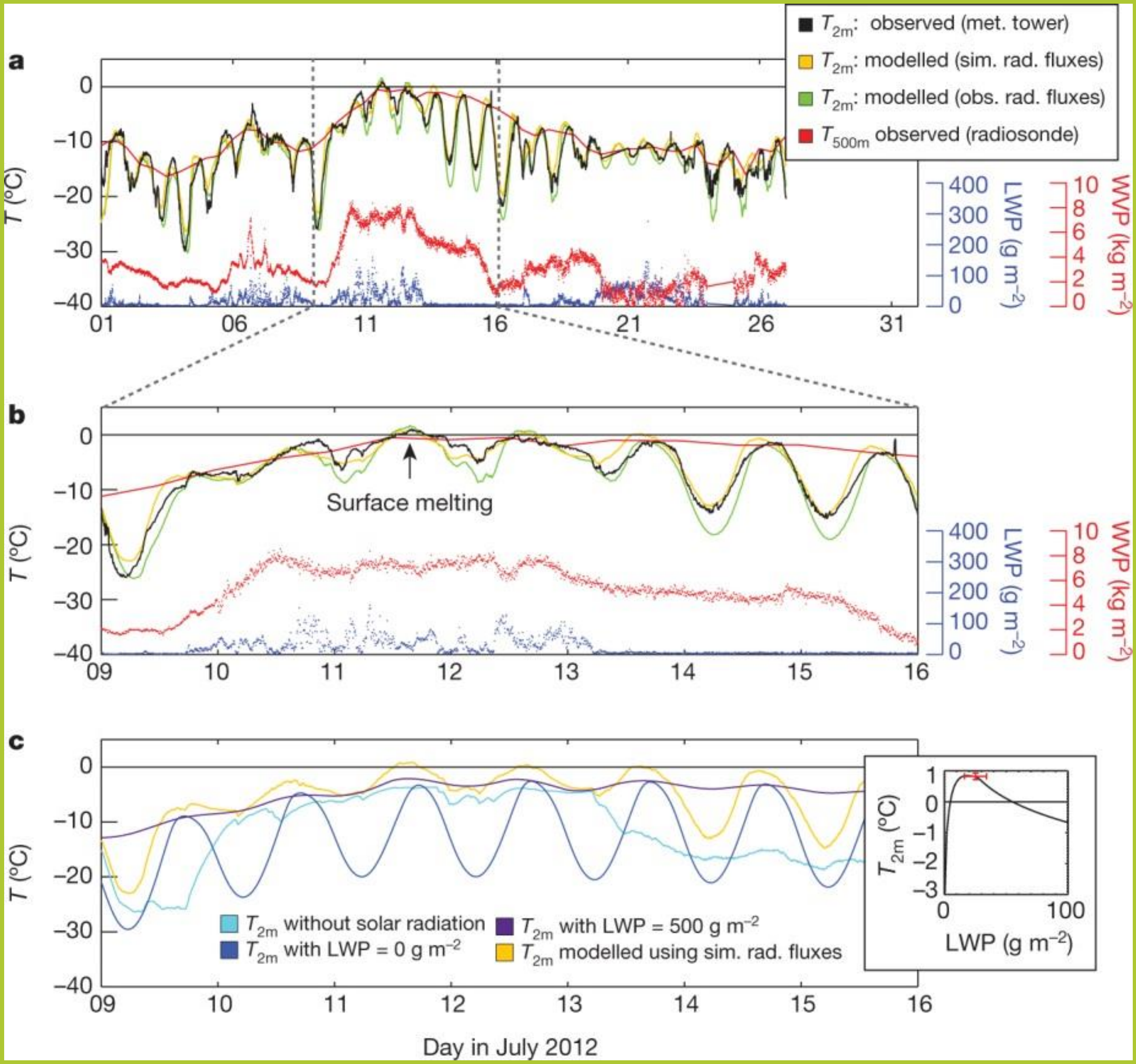

Clouds need to have:

a) Sufficiently large LWP to provide significant increase in LW_d

b) Sufficiently small LWP to allow significant SW_d

i.e., hit LWP "sweet spot" for maximizing surface radiative fluxes, where 'thin, liquid-bearing' clouds are defined as clouds in the range of $10\ g\ m^{-2} < LWP < 60\ g\ m^{-2}$

nature

R Bennartz *et al. Nature* **496**, 83-86 (2013) doi:10.1038/nature12002

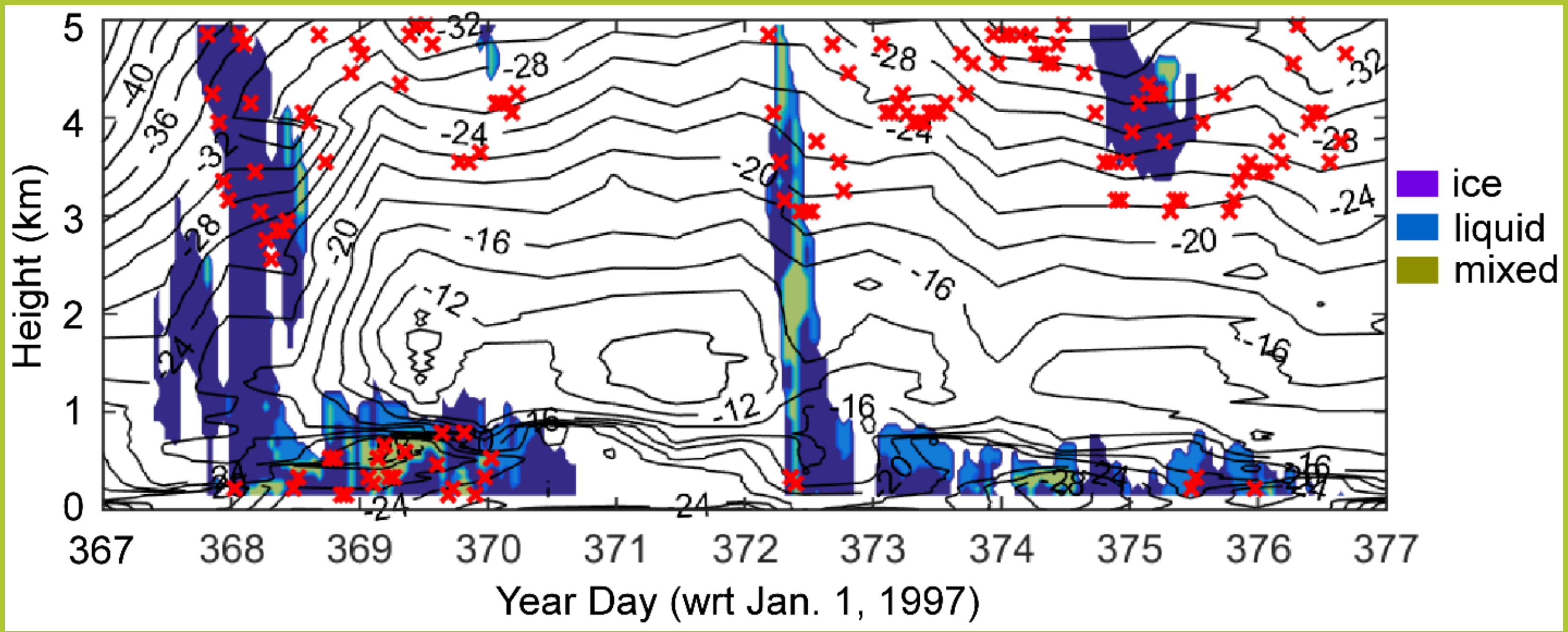
Height (km)
Year Day (wrt Jan. 1, 1997)
ice
liquid
mixed

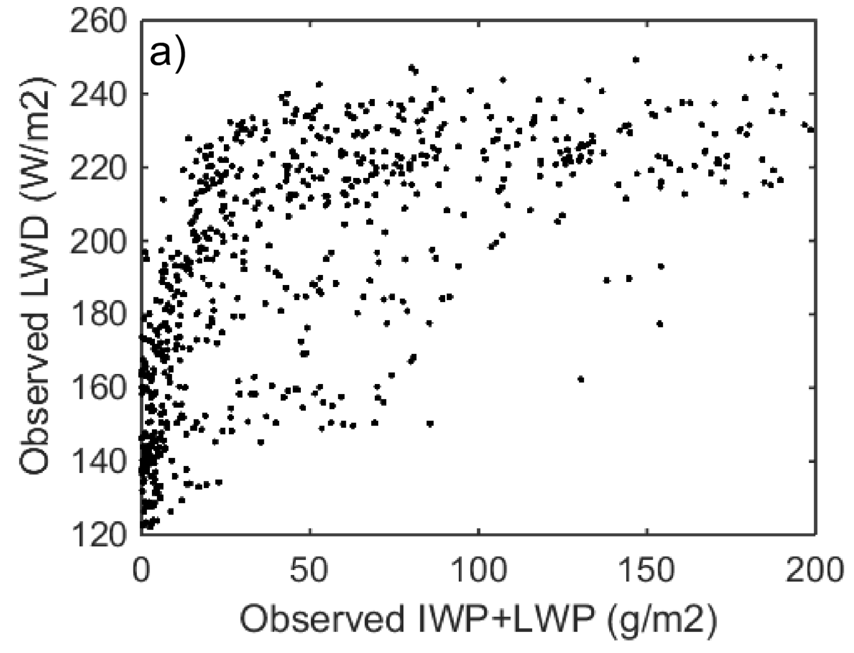
a)
Observed LWD (W/m2)
Observed IWP+LWP (g/m2)

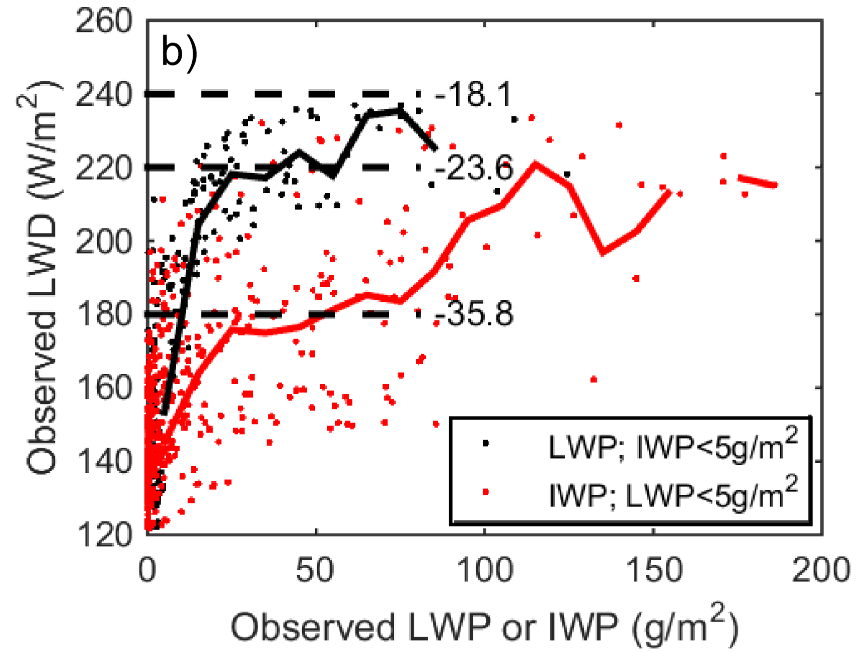
b)
-18.1
-23.6
-35.8
LWP; IWP<5g/m2
IWP; LWP<5g/m2
Observed LWD (W/m2)
Observed LWP or IWP (g/m2)

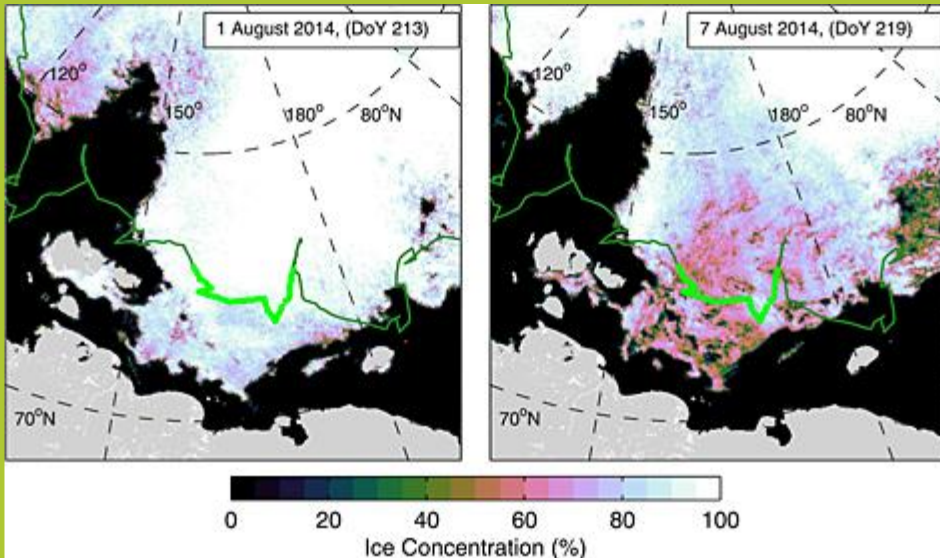

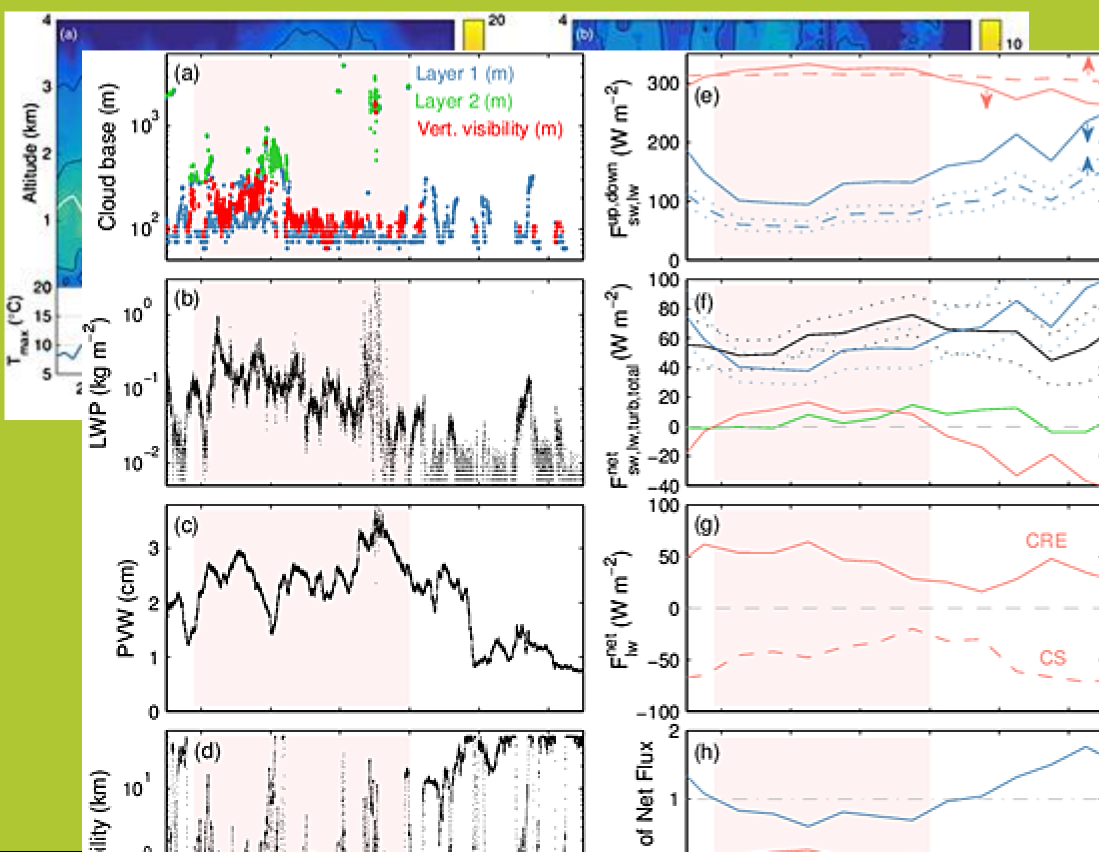

Time series of (a–d) variables related to the clouds and (e–h) daily averaged surface energy fluxes: Figure 6a shows cloud base heights and vertical visibility (m); Figure 6b shows LWP (kg m^{-2}); Figure 6c shows PWV (cm); Figure 6d shows horizontal visibility (km); Figure 6e downwelling (solid) and upwelling (dashed) longwave (red) and solar (blue) radiation; Figure 6f shows net longwave (red) and solar (blue) radiation, and sum of turbulent sensible and latent heat fluxes (green), and total energy flux (black); Figure 6g shows net clear sky longwave (dashed) and surface cloud radiation effect (solid); and Figure 6h shows the net solar (blue), longwave (red), and turbulent (green) heat fluxes as fractions of the total surface energy flux. All energy fluxes are in Wm^{-2}, and except in (e), positive fluxes are downward. Upwelling and net solar radiation and total energy flux assume an albedo of 60%; dotted lines indicate ±10% about this. In Figure 6a, multiple values of cloud base height are given when lowest layers cover less than 100% of the sky: lowest cloud base in blue and second lowest in green, while vertical visibility (red) is only indicated for dense fog. The shaded region indicates the period with positive surface net longwave radiation.

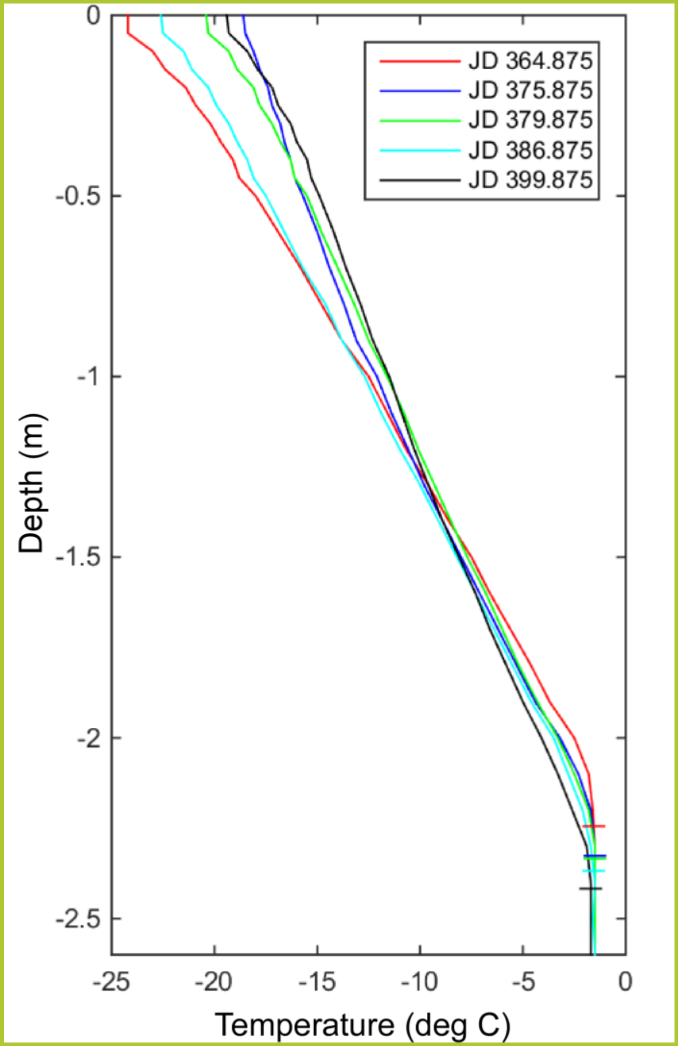

JD 364.875
JD 375.875
JD 379.875
JD 386.875
JD 399.875
Depth (m)
Temperature (deg C)
0
-0.5
-1
-1.5
-2
-2.5
-25
-20
-15
-10
-5
0

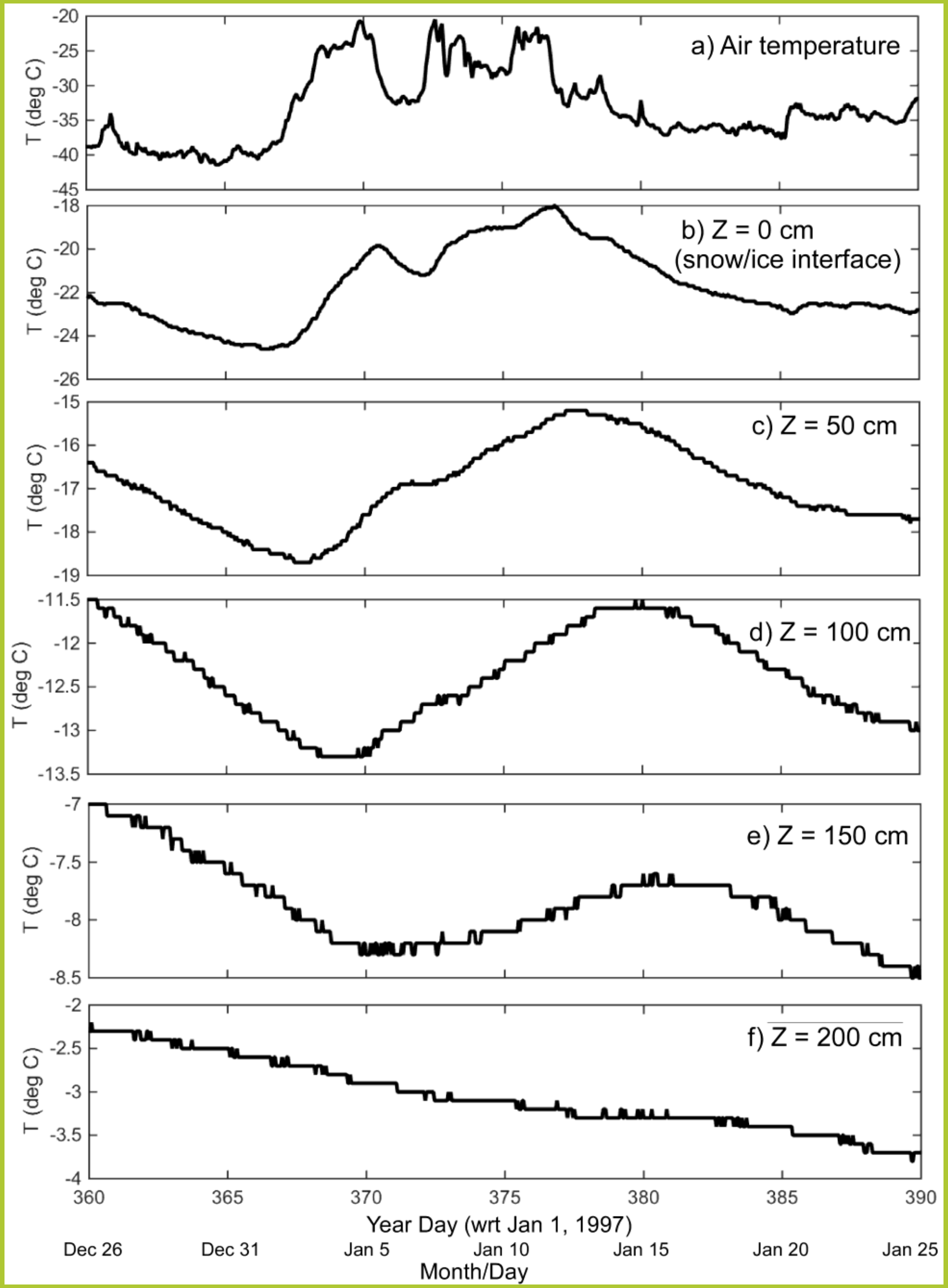

a) Air temperature
b) Z = 0 cm
(snow/ice interface)
c) Z = 50 cm
d) Z = 100 cm
e) Z = 150 cm
f) Z = 200 cm
T (deg C)
360
365
370
375
380
385
390
Year Day (wrt Jan 1, 1997)
Dec 26
Dec 31
Jan 5
Jan 10
Jan 15
Jan 20
Jan 25
Month/Day

SHEBA Jan. 1-12, 1998; Beaufort Sea

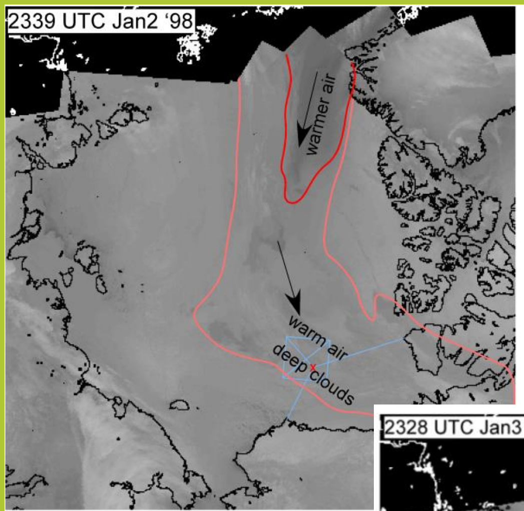

IR satellite images

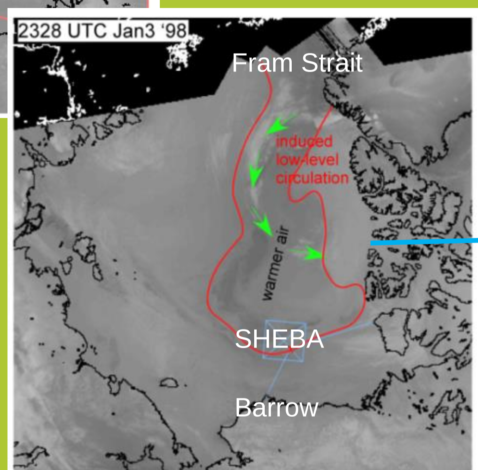

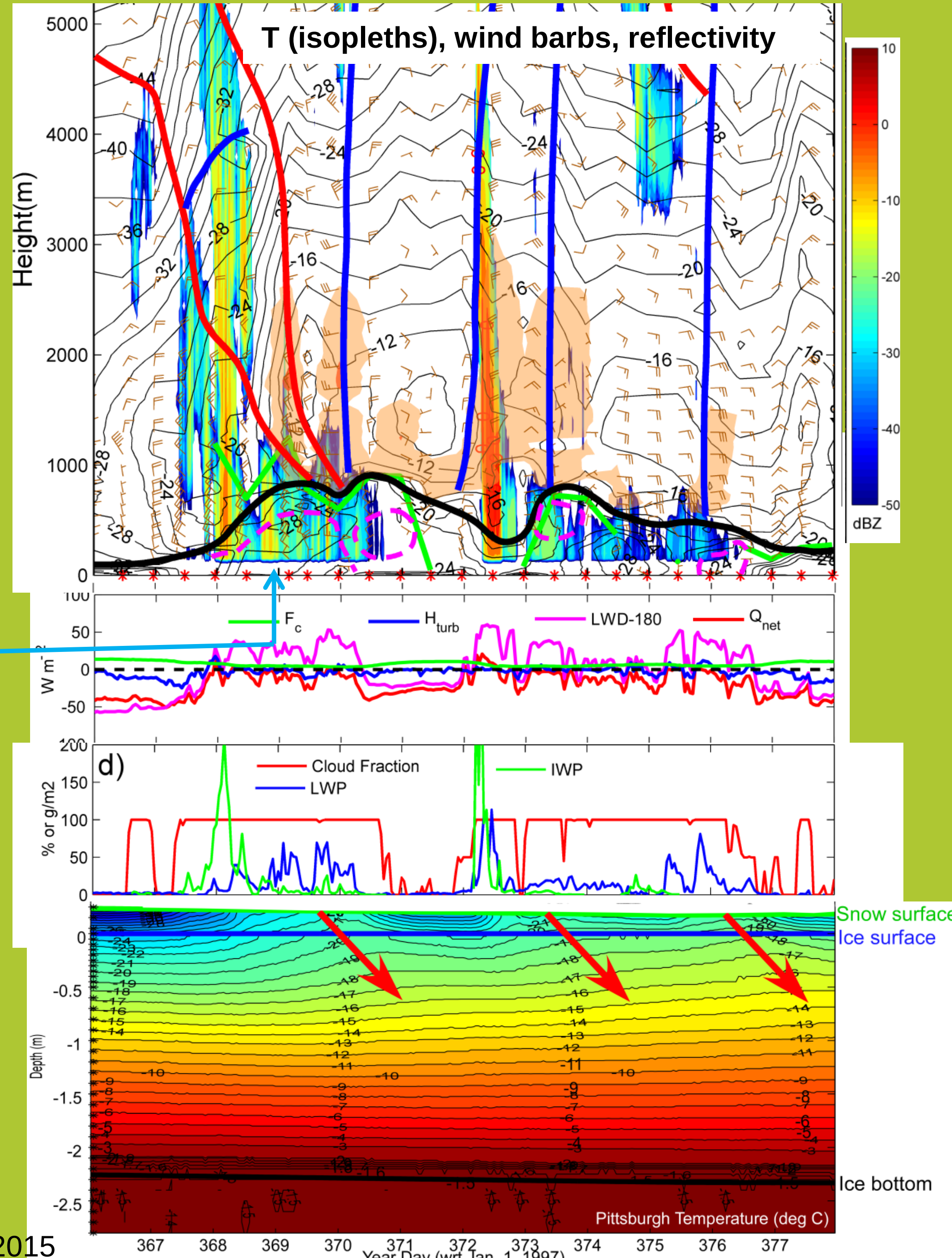

1) Long-distance free tropospheric advection of heat and moisture significant

2) Associated clouds (esp. with liquid) have strong impact on LW_d, F_{net}, and T_s

3) Thermal structure in snow and ice respond strongly to synoptic/mesoscale atmospheric events and presence of liquid water in clouds

Persson et al 2015

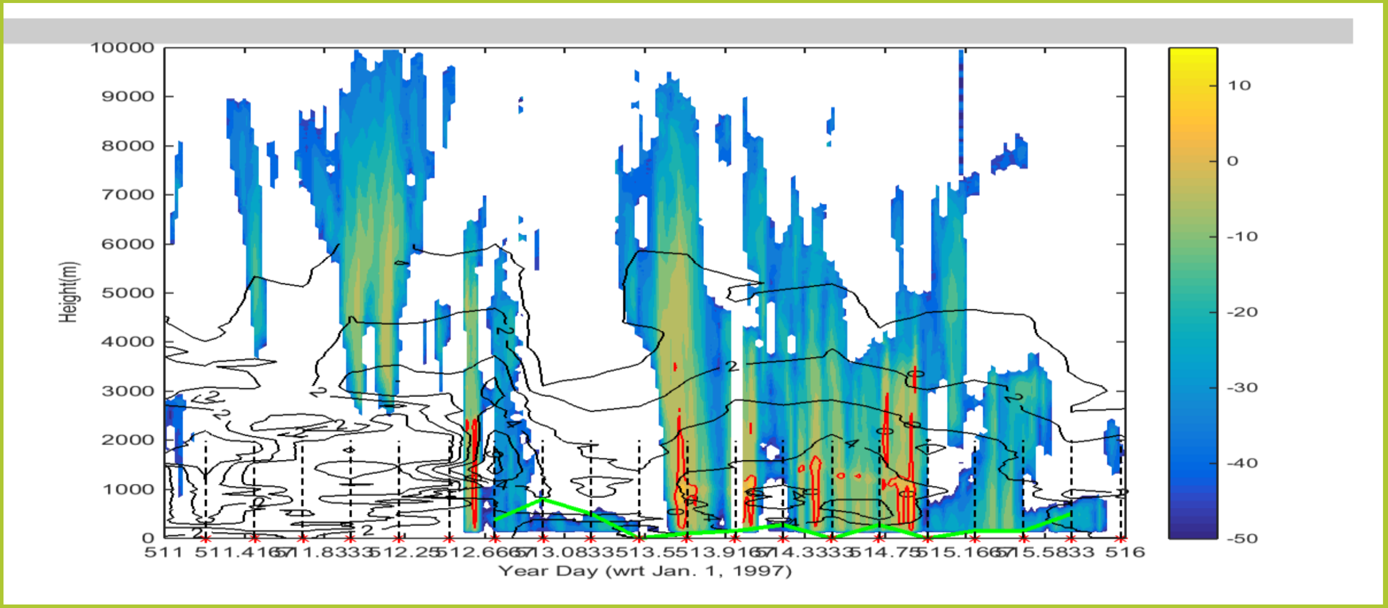

Height(m)
10000
9000
8000
7000
6000
5000
4000
3000
2000
1000
0
511 511.4167 511.8333 512.25 512.6667 513.0833 513.5 513.9167 514.3333 514.75 515.1667 515.5833 516
Year Day (wrt Jan. 1, 1997)
10
0
-10
-20
-30
-40
-50

Arctic Moisture Intrusions

Doyle JG, Lesins G, Thackray CP, Perro C, Nott GJ , Duck TJ, Damoah R , Drummond JR (2011) Water vapor intrusions into the high Arctic during winter. *Geophys. Res. Lett*., **38**, L12806, doi:10.1029/2011GL047493

Persson, P. O. G., M. Shupe, D. Perovich, and A. Solomon, 2016: Linking atmospheric synoptic transport, cloud phase, surface energy fluxes, and sea-ice growth: Observations of midwinter SHEBA conditions. *Clim. Dyn*., In Review.

Woods C, Caballero R, Svensson G (2013) Large-scale circulation associated with moisture intrusions into the Arctic during winter. *Geophys. Res. Lett*., **40**, 4717-4721, doi:10.1002/grl.50912

Neiman et al 2008

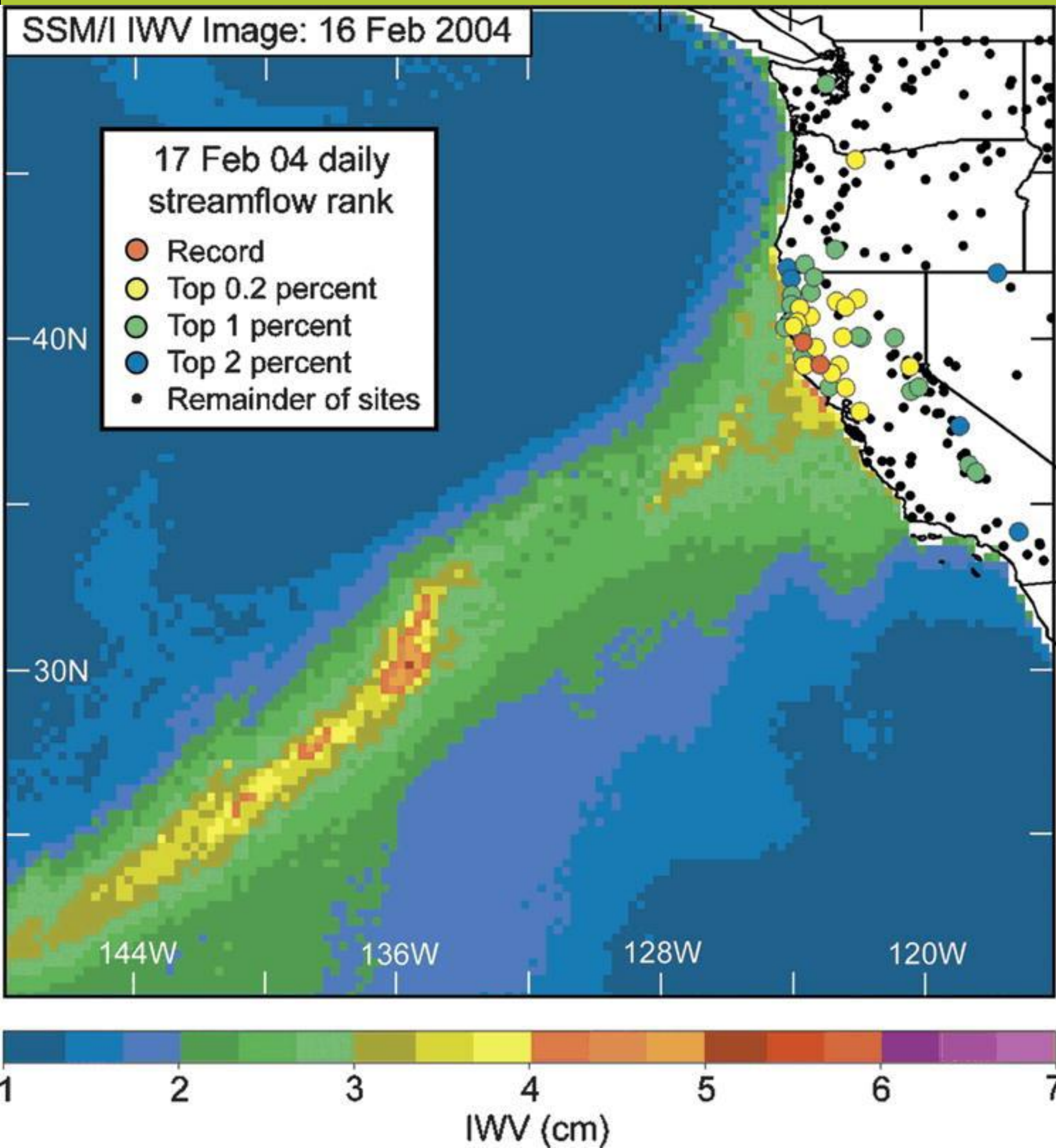

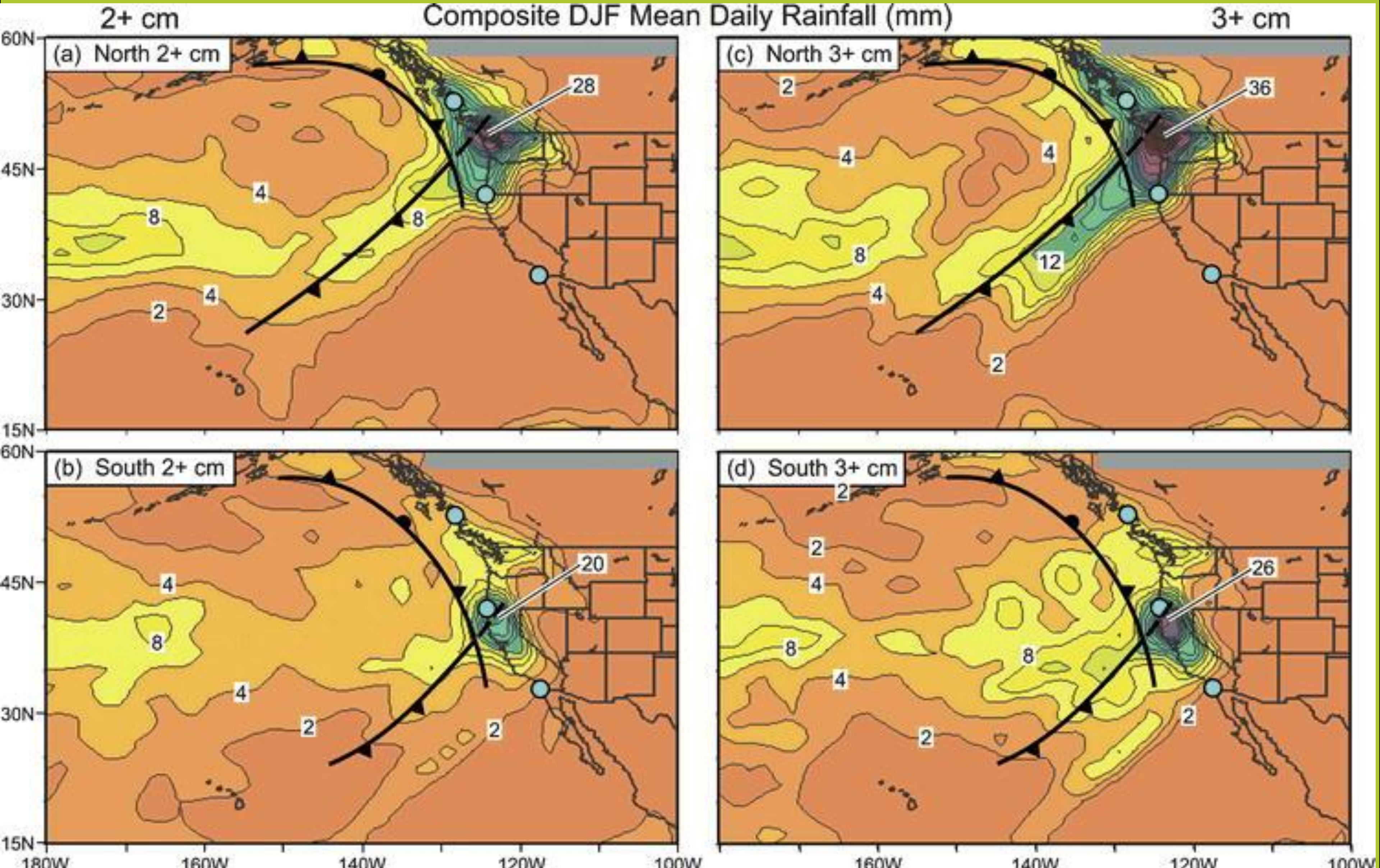
2+ cm
Composite DJF Mean Daily Rainfall (mm)
3+ cm
(a) North 2+ cm
(b) South 2+ cm
(c) North 3+ cm
(d) South 3+ cm
60N
45N
30N
15N
180W
160W
140W
120W
100W
28
36
20
26
12
8
4
2

<u>Atmospheric Rivers</u>:

Newel et al (1992); Zhu and Newell (1998) (Using ECMWF gridded data)

- “water vapor transport in the troposphere is characterized by a filamentary structure, called tropospheric rivers”

- “the moisture flux in a typical tropospheric river is about 1.6 X 10^8 kg s^{-1}, which is similar to the flux in the Amazon River”

- “four or five atmospheric rivers in each hemisphere may carry the majority of the meridional fluxes over the globe”

- “for meridional transport at middle latitudes, the rivers account for substantially all of the transport”

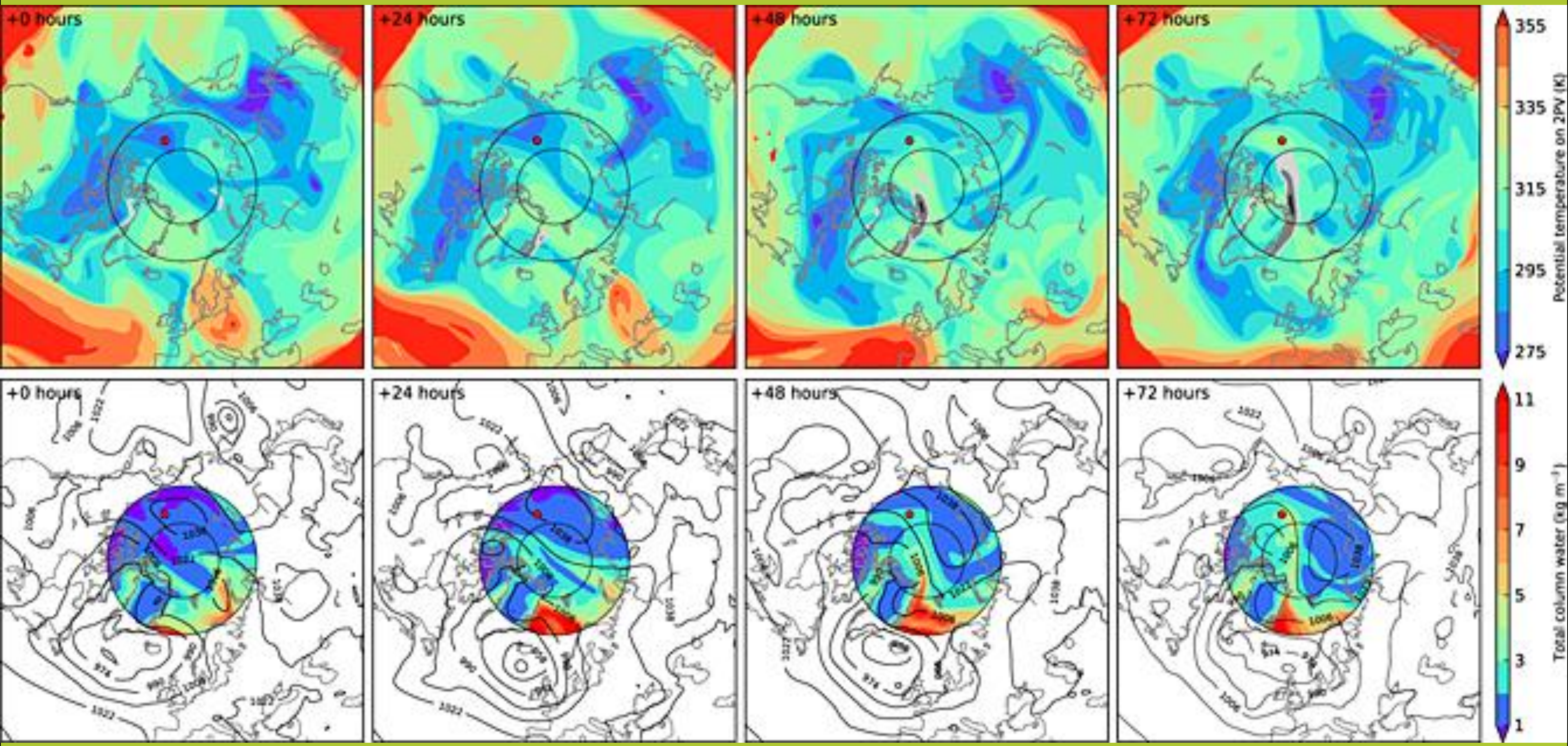
+0 hours
+24 hours
+48 hours
+72 hours
355
335
315
295
275
Potential temperature on 2PV (K)
+0 hours
+24 hours
+48 hours
+72 hours
11
9
7
5
3
1
Total column water (kg m⁻²)

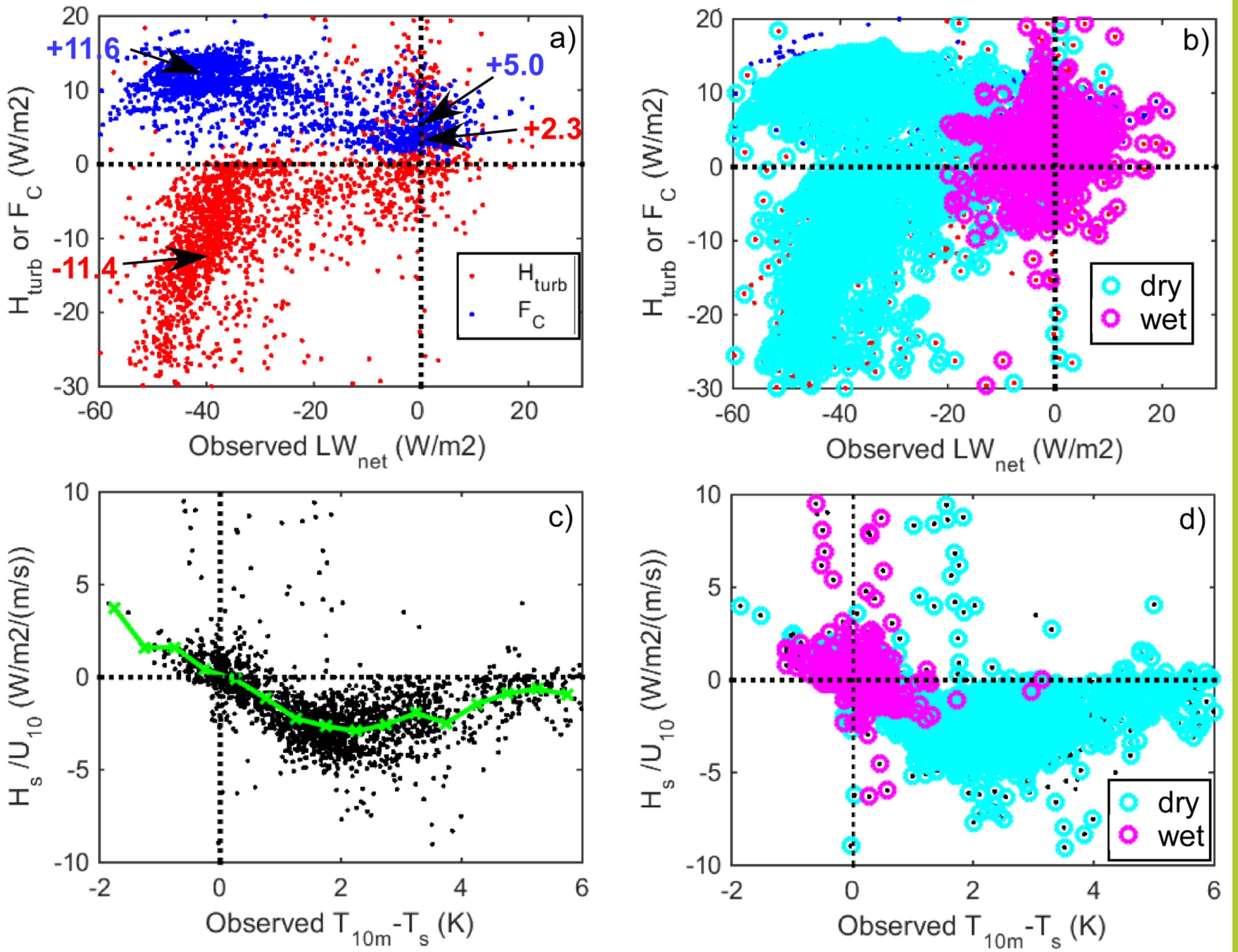
a)
+11.6
+5.0
+2.3
-11.4
H_{turb}
F_C
H_{turb} or F_C (W/m2)
Observed LW_{net} (W/m2)
b)
dry
wet
H_{turb} or F_C (W/m2)
Observed LW_{net} (W/m2)
c)
H_s /U_{10} (W/m2/(m/s))
Observed T_{10m}-T_s (K)
d)
dry
wet
H_s /U_{10} (W/m2/(m/s))
Observed T_{10m}-T_s (K)